Applied Geochemistry 102 (2019) 64–76

Contents lists available at ScienceDirect

Applied Geochemistry

journal homepage: www.elsevier.com/locate/apgeochem

Dating of glacial palaeogroundwater in the Ordovician-Cambrian aquifer system, northern Baltic Artesian Basin

Joonas Pärn[a,b,*], Kristine Walraevens[c], Marc van Camp[c], Valle Raidla[a,b], Werner Aeschbach[d], Ronny Friedrich[e], Jüri Ivask[a], Enn Kaup[a], Tõnu Martma[a], Jonas Mažeika[f], Robert Mokrik[g], Therese Weissbach[d], Rein Vaikmäe[a]

[a] Department of Geology, Tallinn University of Technology, Ehitajate tee 5, 19086, Tallinn, Estonia
[b] Department of Hydrogeology and Environmental Geology, Geological Survey of Estonia, Kreutzwaldi 5, 44314, Rakvere, Estonia
[c] Laboratory for Applied Geology and Hydrogeology, Ghent University, Krijgslaan 281, B-9000 Ghent, Belgium
[d] Institute of Environmental Physics, Heidelberg University, Im Neuenheimer Feld 229, Heidelberg, Germany
[e] Curt-Engelhorn-Center Archaeometry, C4, 8, 68159, Mannheim, Germany
[f] Institute of Geology and Geography, Nature Research Centre, Akademijos Str. 2, LT-08412, Vilnius, Lithuania
[g] Department of Hydrogeology and Engineering Geology, Vilnius University, Čiurlionio 21, 2009, Vilnius, Lithuania

ARTICLE INFO

Editorial handling by Dr F Chabaux

ABSTRACT

The Ordovician-Cambrian aquifer system in the northern Baltic Artesian Basin contains glacial palaeogroundwater that originates from the Scandinavian Ice Sheet that covered the study area in the Pleistocene. Previously, no absolute dating of this palaeogroundwater has been attempted. In this multi-tracer study, we use ^{3}H, ^{14}C, ^{4}He and stable isotopes of water to constrain the age distribution of groundwater. We apply the geochemical modelling approach developed by van der Kemp et al. (2000) and Blaser et al. (2010) to calculate the theoretical composition of recharge waters in three hypothetical conditions: modern, glacial and interstadial for ^{14}C model age calculations. In the second phase of the geochemical modelling, the calculated recharge water compositions are used to calculate the ^{14}C model ages using a series of inverse models developed with NETPATH. The calculated ^{14}C model ages show that the groundwater in the aquifer system originates from three different climatic periods: (1) the post-glacial period; (2) the Late Glacial Maximum (LGM) and (3) the pre-LGM period. A larger pre-LGM component seems to be present in the southern and north-eastern parts of the aquifer system where the radiogenic ^{4}He concentrations are higher (from $\sim 3.0 \cdot 10^{-5}$ to $5.5 \cdot 10^{-4}$ cc·g^{-1}) and the stable isotopic composition of water is heavier ($\delta^{18}O$ from −13.5‰ to −17.3‰). Glacial palaeogroundwater from the north-western part of the aquifer system is younger and has ^{14}C model ages that coincide with the end of the LGM period. It is also characterized by lower radiogenic ^{4}He concentrations ($\sim 2.0 \cdot 10^{-5}$ cc·g^{-1}) and lighter stable isotopic composition ($\delta^{18}O$ from −17.7 to −22.4‰). Relations between radiogenic ^{4}He and ^{14}C model ages and between radiogenic ^{4}He and Cl^{-} concentration show that groundwater in the aquifer system does not have a single well-defined age. Rather, the groundwater age distribution has been influenced by mixing between waters originating from end-members with strongly differing ages. Overall the results suggest, that in the shallower northern part of the aquifer system, significant changes in groundwater composition can be brought about by glacial meltwater intrusion during a single glaciation. However, multiple cycles of glacial advance and retreat are needed to transport glacial meltwater to the deeper parts of the aquifer system.

1. Introduction

More than half of total aquifer storage in the Earth's upper crust is occupied by groundwater that has renewal periods greatly exceeding the human life-span (Gleeson et al., 2010, 2016; Jasechko et al., 2017). Groundwater that originates from water cycles under environmental conditions which are different from the present can be defined as palaeo(ground)water (Fontes, 1981). The preservation of palaeogroundwater can be related to several factors such as confinement by thick aquitards, dry climate conditions with small amounts of modern recharge and low hydraulic conductivity that results in low actual velocity of groundwater (Clark and Fritz, 1997). It is critical to sustainably

* Corresponding author. Department of Geology at Tallinn University of Technology, Ehitajate tee 5, 19086, Tallinn, Estonia
E-mail address: joonas.parn@taltech.ee (J. Pärn).

https://doi.org/10.1016/j.apgeochem.2019.01.004
Received 11 July 2018; Received in revised form 9 January 2019; Accepted 11 January 2019
Available online 15 January 2019
0883-2927/

manage palaeogroundwater resources, as present-day groundwater abstraction may only partially be compensated by modern recharge if at all. Water yields and quality may greatly deteriorate with over-exploitation of palaeogroundwater. The first step towards a responsible and sustainable management of groundwater resources is the determination of their age and renewal periods.

Glacial palaeogroundwater in the northern part of the Baltic Artesian Basin (BAB) is a unique groundwater resource that originates from glacial meltwater recharge in the Pleistocene. It has been shown by numerical modelling that aquifers in sedimentary basins in formerly glaciated areas had sufficient transmissivity to discharge subglacial meltwater (e.g. Boulton et al., 1995; Lemieux et al., 2008; Sterckx et al., 2017, 2018). Significantly higher heads imposed by continental ice sheets compared to modern topographically driven heads were able to reverse the regional groundwater flow (Person et al., 2007; McIntosh et al., 2011). The reorganisation of groundwater flow is evident from the isotopic and chemical composition of the groundwater which is in many cases out of equilibrium with modern topographically driven flow patterns (Stueber and Walter, 1991, 1994; Grasby et al., 2000). The presence of glacial palaeogroundwater in the northern BAB is exemplified by the lightest $\delta^{18}O$ values found in Europe ranging from −18.5 to −23.0‰ (Vaikmäe et al., 2001; Raidla et al., 2009; Pärn et al., 2016).

Currently, the glacial palaeogroundwater is used extensively for public water supply in northern Estonia. The glacial component in these waters is essentially non-renewable and modern recharge into the aquifer systems remains limited. To date, much of the work on glacial palaeogroundwater in the BAB has concentrated on the deepest Cambrian-Vendian aquifer system (Vaikmäe et al., 2001; Raidla et al., 2009, 2012, 2014; Gerber et al., 2017). This is essentially a fossil aquifer system where the influence of modern groundwater recharge is minimal and confined to very restricted areas in its northern part. Previous ^{14}C age estimates (Raidla et al., 2012) suggested that the recharge of glacial meltwater into the Cambrian-Vendian aquifer system was coeval with the advance and maximum extent of Scandinavian Ice Sheet during Late Weichselian Glaciation in the Late Pleistocene (~14–27 ka BP).

The overlying Ordovician-Cambrian (O-Cm) aquifer system is more influenced by modern groundwater recharge (Pärn et al., 2016, 2018). Nevertheless, in large areas a substantial glacial component in groundwater is still present. This is exemplified by the fact, that in the modern recharge area of the aquifer system the isotopic composition of groundwater is significantly depleted ($\delta^{18}O$ values from −14 to −17‰; Pärn et al., 2016) with respect to both values found in modern precipitation (~ −10.3‰; IAEA/WMO, 2018) and in shallow groundwater (−11.5 to −12.5‰; Raidla et al., 2016). The fraction of glacial palaeogroundwater becomes larger farther down the groundwater flow path as indicated by $\delta^{18}O$ values decreasing down to −22‰ (Pärn et al., 2016). However, the age of glacial palaeogroundwater in the O-Cm aquifer system has not been studied.

Despite various reported problems (e.g. Sanford, 1997; Geyh, 2000; Aeschbach-Hertig et al., 2002; Aggarwal et al., 2014), radiocarbon dating (^{14}C) has the most suitable half-life to study groundwater recharged in the Holocene and Late Pleistocene with ages up to 30 ka BP and is still widely used in hydrogeologic studies in conjunction with other age tracers (e.g. Blaser et al., 2010; Plummer et al., 2012; Grundl et al., 2013; Cendón et al., 2014; Vautour et al., 2015; Petersen et al., 2018). However, several preconditions have to be met for a successful interpretation of ^{14}C activities ($a^{14}C$) in terms of age (Kalin, 2000; Plummer and Glynn, 2013). Among the most important is the estimation of initial activity of radiocarbon of the recharge waters (A_0) at the point where infiltrating water is isolated from the soil carbon reservoir. Also, chemical and physical processes farther down the flow path that change the initial A_0 value need to be quantified. This comprises the dilution of initial A_0 due to the dissolution of carbonate minerals both in the soil and the saturated zone which is accompanied by isotopic exchange reactions and matrix exchange. Furthermore, the addition of ^{14}C-free dissolved inorganic carbon (DIC) from the oxidation of organic matter and methanogenesis has to be accounted for in interpreting ^{14}C activities in terms of age (e.g. Aravena et al., 1995a, b). Several correction models have been developed to quantify the effects of such chemical processes on the DIC pool and A_0 value (e.g. Tamers, 1975; Fontes and Garnier, 1979; Plummer et al., 1983, 1990; van der Kemp et al., 2000; Coetsiers and Walraevens, 2009; Blaser et al., 2010; Han and Plummer, 2013). In addition, an assessment has to be made for possible contamination of ^{14}C samples with atmospheric CO_2 during sampling or during the transfer of the sample to a gas extraction system (Aggarwal et al., 2014).

In this contribution, we aim to constrain the age distribution of groundwater in the O-Cm aquifer system by using ^{14}C as the main tracer. The O-Cm aquifer system contains groundwater with various recharge histories for which the initial parameters of recharge waters (e.g. A_0 and $\delta^{13}C_{rech}$) in the modern recharge environment cannot be applied and have to be estimated using geochemical modelling. We use a hydrochemical model developed by van der Kemp et al. (2000) and Blaser et al. (2010) that considers different climate conditions (e.g. initial pCO_2, temperature) during groundwater recharge to estimate the initial parameters for recharge waters. The ^{14}C model age is calculated using NETPATH (Plummer et al., 1994; El-Kadi et al., 2011). A groundwater sample is essentially a mixture of many flow paths with different ages that is characterized by an age distribution rather than a single unique age (e.g. Varni and Carrera, 1998; Corcho Alvarado et al., 2007; McCallum et al., 2014; Suckow, 2014). This is important to consider in the O-Cm aquifer system as mixing between groundwater with different origin has been shown to be an important process here (Pärn et al., 2016). To better characterize the age distribution of groundwater in the O-Cm aquifer system, the interpretation of calculated ^{14}C model ages is complemented by age estimates provided by ^{3}H activities, radiogenic ^{4}He concentrations and $\delta^{18}O_{water}$ values. Previously published ^{81}Kr ages from the southern part of the aquifer system (Gerber et al., 2017) are also considered.

2. Geology and hydrogeological setting

The O-Cm aquifer system is a confined water body in the northern part of the BAB (Fig. 1). It is hosted by sandstones and siltstones of Cambrian and Early Ordovician age. The rocks forming the O-Cm aquifer system are distributed in most of the northern BAB, except in a narrow coastal region of northern Estonia (Fig. 1). The thickness of the aquifer system increases from 20 m in northern Estonia to ~120 m in Latvia (Juodkazis, 1980; Savitskaja et al., 1995; Perens and Vallner, 1997). The depth of the strata forming the aquifer system is 10–20 m below ground surface in northern Estonia and increases southward to over 1000 m in Latvia and Lithuania. Sandstones forming the matrix of the aquifer system are weakly cemented quartz arenites or subarkoses, with quartz content up to 90% (Raidla et al., 2006). The cement consists mainly of Fe-dolomite whose abundance is 3% on average (Raidla et al., 2006). In addition, the upper portion of the sandstone formation contains accessory phosphorite (authigenic apatite). The lateral hydraulic conductivity of the sandstone ranges from 1 to 3 $m\,d^{-1}$ (Perens and Vallner, 1997). Transmissivity ranges from 25 to 50 $m^2\,d^{-1}$ in northern Estonia and from 80 to 130 $m^2\,d^{-1}$ in southern Estonia due to the increased thickness of the aquifer system in the south (Savitskaja et al., 1995; Perens and Vallner, 1997). The aquifer is confined from above by the Silurian-Ordovician regional aquitard composed of limestones, dolomites, marls, siltstones, clays and black shale (graptolite argillite) with transversal hydraulic conductivity that ranges from 10^{-7} to 10^{-5} $m\,d^{-1}$ (Perens and Vallner, 1997). The underlying Lükati-Lontova regional aquitard, consisting of siltstones and clays of the Lower Cambrian age, separates the O-Cm aquifer system from the Cambrian-Vendian aquifer system and has a transversal hydraulic conductivity of ~10^{-7} $m\,d^{-1}$ (Perens and Vallner, 1997).

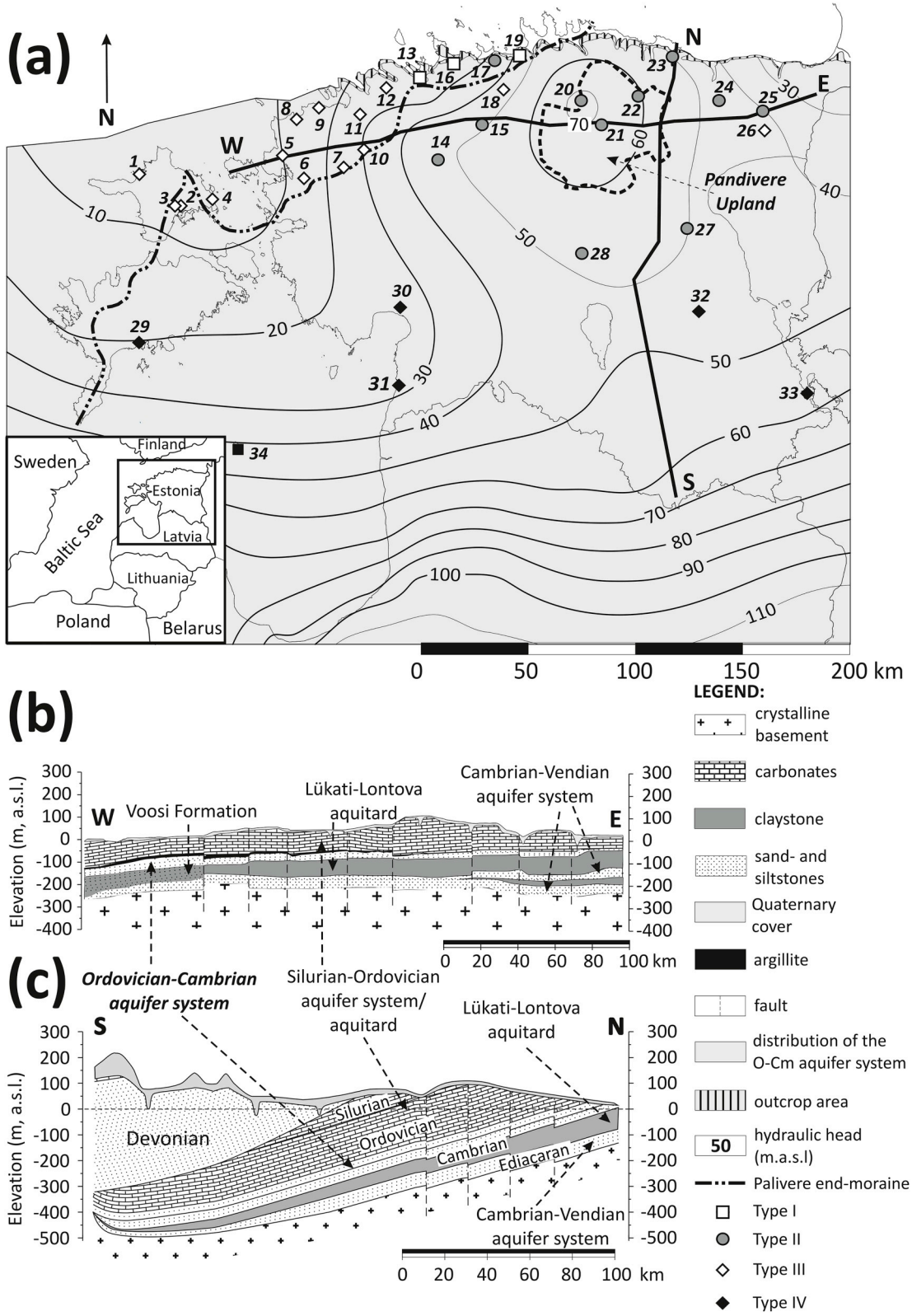

Fig. 1. (a) Location and distribution of the Ordovician-Cambrian (O-Cm) aquifer system in the northern Baltic Artesian Basin (BAB) together with the distribution of pre-development freshwater heads (m., a.s.l.). The freshwater heads are calculated based on hydraulic head measurements given in Tšeban (1966) and Takcidi (1999). The distributions of the outcrop area of the aquifer system together with the location of Pandivere Upland and the location of the Palivere end-moraine formed during the Late Glacial period (~12.7–14.7 ka BP; Kalm, 2006) are shown for reference. Numbers and symbols denote the position of sampling points in Table S1 (Supplementary material). The water types are explained in Section 5.3. (b) the west-east cross-section of northern BAB; (c) the north-south cross-section of the northern BAB.

Groundwater in the O-Cm aquifer system can be classified into three general groundwater types (Pärn et al., 2016). In the northern margin of the aquifer system, near the outcrop area of the aquifer forming rocks, Ca-HCO_3 type groundwater can be found with an isotopic composition similar to shallow aquifers (−11.5 to −12.5‰; Pärn et al., 2016; Raidla et al., 2016). In these areas the thickness of overlying Ordovician carbonate formation is small (< 20 m; Fig. 1a, c). A second type of groundwater occupies areas farther away from the outcrop area of the aquifer system, where the overlying thickness of carbonate formation is larger (see Fig. 1c). These waters have a significantly depleted isotopic composition ($\delta^{18}O$ values from −14 to −22.5‰; Pärn et al., 2016) with respect to values found in Ca-HCO_3 type groundwater. The groundwater is characterized by low TDS concentrations (from 200 to 600 mg L^{-1}) and a Na-HCO_3 water type due to cation exchange reactions (Pärn et al., 2016). These waters represent glacial palaeogroundwater, that have evolved from glacial meltwater originating from the Scandinavian Ice Sheet that intruded the aquifer system in the Pleistocene (Pärn et al., 2016; Sterckx et al., 2018). The freshening of aquifers and the emergence of a related Na-HCO_3 water type due to glacial meltwater intrusion has previously been reported from various sedimentary basins in North America (e.g. McIntosh and Walter, 2006; Ferguson et al., 2007; Cloutier et al., 2010). The third type of groundwater can be found in the deeper southern parts of the aquifer system. Here, groundwater evolves from brackish groundwater to brine with increasing depth and its water type changes to Na-Cl and Na-Ca-Cl. The high freshwater heads observed in the deeper parts of the aquifer system (Fig. 1) are mainly due to very high salinity (TDS up to ~150 g L^{-1}). The brackish groundwater in the aquifer system has developed through mixing between saline formation waters and glacial palaeogroundwater evolved from glacial meltwater intrusion in the Pleistocene (Pärn et al., 2016; Gerber et al., 2017). This is exemplified by depleted $\delta^{18}O$ values in brackish groundwater (from −9 to −17.3‰) with respect to values found in brine from the deeper parts of the BAB ($\delta^{18}O$ ~ −4.5‰, Babre et al., 2016; Gerber et al., 2017).

3. Material and methods

The study is based on groundwater samples from 33 water supply and observation wells screened in the O-Cm aquifer system in Estonia, collected during two fieldwork campaigns undertaken in 2015 and 2016. In 2015, samples were collected for hydrochemical, stable isotope (δ^2H, $\delta^{18}O$, $\delta^{13}C$), age tracer ($a^{14}C$, ^3H) and noble gas (He, Ne) measurements. Additional fieldwork was carried out in 2016 at the same sampling points to collect samples for $a^{14}C$ AMS measurements, accompanied by samples for hydrochemical and stable isotope (δ^2H, $\delta^{18}O$, $\delta^{13}C$) analysis. The study also uses He and Ne data from Weissbach (2014). The data set interpreted in this study together with references to previously published data are given in Table 2 and Tables S1 and S2 (Supplementary material).

The sample collecting procedure in the field is characterized in detail in Pärn et al. (2018). HCO_3^- and CO_3^{2-} concentrations were measured in the Laboratory of the Geological Survey of Estonia using the titration method (ISO 9963–1; analytical precision of ± 3%) and in the field using a Millipore MColortest™ titration kit (analytical precision of ± 11 mg L^{-1}) in 2015 and 2016, respectively. Major and minor ion concentrations were measured in the Department of Geology at Tallinn University of Technology using a Thermo Dionex ICS-1100 ion chromatograph. The analytical precision for major and minor ionic components was ± 0.5–2.6% and ± 1.3–4.3%, for cations and anions, respectively, depending on the ions measured (Table S1). Fe^{2+} and Mn^{2+} concentrations for samples collected in 2016 were determined in the Laboratory for Applied Geology and Hydrogeology at Ghent University using atomic adsorption spectrometry (Table S1; analytical precision of ± 0.05 mg L^{-1}).

Stable isotope ratios of hydrogen and oxygen in water and the carbon isotope composition of DIC were analysed in the Laboratory of mass spectrometry at the Department of Geology, Tallinn University of Technology (Table S2). Isotope ratios of hydrogen and oxygen are expressed in standard δ-notation relative to the Vienna Standard Mean Ocean Water (V-SMOW). Isotope ratios of hydrogen and oxygen were measured using a Picarro L2120-i Isotopic Water Analyzer (Brand et al., 2009). Reproducibility of the stable isotope measurements was ± 0.1‰ for $\delta^{18}O$ and ± 1‰ for δ^2H. The carbon isotope composition of DIC ($\delta^{13}C_{DIC}$) was determined using a Thermo Fisher Scientific Delta V Advantage mass spectrometer from DIC precipitated as $BaCO_3$ (Clark and Fritz, 1997; Table S2). For samples collected in 2015 the $\delta^{13}C_{DIC}$ values were determined from $BaCO_3$ precipitated together with samples for ^{14}C determination from volumes of 150–250 L. For samples collected in 2016 the $\delta^{13}C_{DIC}$ was determined from $BaCO_3$ precipitates prepared in 1 L glass bottles (Table S2). The results are expressed in ‰ deviation relative to Vienna Peedee Belemnite (V-PDB). Reproducibility of $\delta^{13}C$ of the internal laboratory standards was better than ± 0.1‰. The reproducibility of $\delta^{13}C_{DIC}$ was better than ± 0.4‰ based on $BaCO_3$ precipitates collected as duplicate and triplicate samples (Pärn et al., 2018; Table S2).

The samples for the measurement of radiocarbon activities ($a^{14}C$) were collected during two fieldwork campaigns in 2015 and 2016. In 2015 radiocarbon activities were measured with the conventional method in the Radiocarbon Laboratory of the Department of Geology at Tallinn University of Technology. The samples were collected into a number of vessels with a total volume from 150 to 250 L from which DIC was precipitated as $BaCO_3$ and synthesized to benzene for liquid scintillation counting (Clark and Fritz, 1997). The radiocarbon activity of the samples was determined with Quantulus 1220 liquid scintillation spectrometer. The ^{14}C activities are reported as percentage of the modern standard (pmC). The analytical precision for radiocarbon activity measurements is estimated to be ± 0.5 pmC, based on duplicate and triplicate samples collected in 2015 and 2016 (Table S2). In 2016, 24 new ^{14}C samples were collected for $a^{14}C$ measurements by AMS. Glass bottles (1 L) submerged in an overflowing container were filled with a small headspace and stabilized with ~1 g of $AgNO_3$ immediately to stop the bacterial activity. In the Institute of Environmental Physics at the Heidelberg University, Germany, acid (5 ml, 3 N HCl) was added to about 100 ml of the water to convert the DIC to CO_2, which was then extracted under vacuum and collected in a glass ampoule (Kreuzer, 2007). The collected CO_2 was then converted into graphite by a custom build graphitisation system. The $a^{14}C$ of the samples was measured by AMS (MICADAS system) at the Curt-Engelhorn-Centre Archaeometry in Mannheim, Germany. The measurement error for the activity of radiocarbon determined by AMS ranged from ± 0.02 to ± 0.2 pmC

Table 1
pCO_2 values and temperature range considered in calculating initial water compositions with the PHREEQC together with the system conditions considered for calcite dissolution (open - isotopically and chemically open; open/closed - chemically open and isotopically closed; closed - isotopically and chemically closed; see also Appendix B in Supplementary material).

Recharge conditions	Recharge temperature (°C)	Initial pCO_2 (atm)	System conditions for calcite dissolution
Glacial	2	$10^{-3.2}$–$10^{-2.4}$	closed
Interstadial	2–4	$10^{-3.7}$–$10^{-2.6}$	open; open/closed; closed
Modern	6	$10^{-2.5}$–$10^{-1.8}$	open; open/closed; closed

(Table S2).

Tritium samples were measured in the Laboratory of Nuclear Geophysics and Radioecology at the Nature Research Centre at Vilnius, Lithuania. The samples were counted with electrolytical enrichment using Quantulus 1220 liquid scintillation spectrometer. ^{3}H concentrations are reported in tritium units (TU) with the detection limit of measurements being 0.2 TU (Table S2). For samples where ^{3}H concentrations exceeded the detection limit, the measurement error was ± 0.2 TU.

Noble gas samples were collected into copper tubes fixed on aluminium racks (Aeschbach-Hertig and Solomon, 2013) during two fieldwork campaigns in 2013 (Weissbach, 2014) and 2015. These copper tubes contained about 20 g of water and were closed vacuum tight by stainless steel clamps. Noble gas contents were determined at the Institute of Environmental Physics at Heidelberg University with a GV Instruments MM 5400 mass spectrometer. The concentrations of He and Ne (calculated from ^{20}Ne, assuming an atmospheric isotopic abundance of 90.5%) were measured with an average analytical precision of ± 1.1% and ± 0.5%, respectively. The precision of the ^{3}He measurement and thus the $^{3}He/^{4}He$ ratio was typically ± 3–5%. However, most of the samples taken in 2015 were affected by an experimental problem that prevented reliable results for ^{3}He (Table 2). For these samples, the reduction of the He amount necessary to bring ^{4}He into the measurable range was so strong that ^{3}He signals became too weak and the corresponding peak was not found.

4. Geochemical modelling

For calculating ^{14}C model ages, we applied geochemical modelling concept that is based on the framework developed by van der Kemp et al. (2000) and Blaser et al. (2010). Previous studies have shown that the O-Cm aquifer system contains groundwater originating from three different end-members (Pärn et al., 2016, Section 2): (1) groundwater originating from modern precipitation, (2) groundwater originating from glacial meltwater intrusion from the Scandinavian Ice Sheet and (3) groundwater originating from saline formation water and brine from the deeper parts of the basin. Thus, modern climatic conditions do not characterize the environmental characteristics (temperature, pCO_2) of the recharge environment for most of the studied waters. In these circumstances the chemical and isotopic composition of modern groundwater cannot be used as a starting point for deriving ^{14}C model ages for groundwater in the aquifer system. We used geochemical modelling with PHREEQC to calculate the isotopic (A_0 and $\delta^{13}C_{rech}$) and chemical composition of recharge waters formed in different recharge conditions. We considered three types of recharge conditions for the O-Cm aquifer system for this modelling exercise: modern, glacial and interstadial. The plausible values for general parameters describing each recharge environment (temperature, pCO_2) are summarized in Table 1. A more detailed discussion on the choice of these values can be found in Supplementary material (Appendix A).

The DIC concentrations and $\delta^{13}C_{rech}$, A_0 values in recharge waters are not only determined by temperature and pCO_2 in the soil zone but also by dissolution of carbonate minerals, most commonly calcite. The dissolving calcite in the study area is ^{14}C-free as the carbonate rocks overlying the O-Cm aquifer system are of Palaeozoic age (Ordovician and Silurian; Fig. 1b and c). Due to the fact, that the rocks forming the O-Cm aquifer system have a very narrow outcrop area, it can be assumed that waters recharging the aquifer system both in the Pleistocene and in the Holocene first came into contact with the overlying carbonate formations. We considered three types of system conditions (open - chemically and isotopically open; open/closed - chemically open and isotopically closed; closed - chemically and isotopically closed) for calcite dissolution in modern and interstadial recharge conditions, while only closed system conditions were considered for glacial conditions for meltwaters recharged under the Scandinavian Ice Sheet (cf. van der Kemp et al., 2000; Blaser et al., 2010, Table 1). Specific details about the calculation of the chemical and isotopic composition of recharge waters can be found in Supplementary material (Appendix B; Tables S4 and S5).

To calculate the ^{14}C model ages, several hydrochemical processes that affect the $a^{14}C$ of DIC in groundwater, in addition to calcite dissolution, were considered for recharge waters. Previous studies have shown that the major processes affecting hydrochemical evolution of groundwater in the O-Cm aquifer system are dissolution of carbonate minerals (i.e. calcite and dolomite), along with cation exchange and oxidation of organic matter (Pärn et al., 2016, 2018). The saturation indices with respect to both calcite and dolomite calculated using PHREEQC (Table S1) suggest that the majority of waters in the aquifer system are in equilibrium with respect to calcite ($SI_{calcite}$ from −0.40 to 0.22) and undersaturated or in equilibrium with respect to dolomite ($SI_{dolomite}$ from −1.13 to 0.36; Table S1, Fig. 2a and b). This suggests that the dissolution of carbonate minerals in the aquifer system takes place mainly in the form of incongruent dissolution of dolomite where calcite is precipitated as dolomite is dissolved. This inference is further supported by increasing Mg/Ca values (up to ~1.5) with increasing DIC concentrations (Fig. 2c). The palaeogroundwater dominant in the northern part of the aquifer system has a Na-HCO_3 water type due to cation exchange reactions of the freshening type (Pärn et al., 2016). Cation exchange reactions cause secondary dissolution of carbonate minerals as Ca^{2+} is removed from the solution, which can lead to a further dilution of the ^{14}C-active component in DIC (Appelo and Postma, 2005). Previous studies (Raidla et al., 2012) and data from laboratory experiments with Cambrian and Lower Ordovician sedimentary rocks have shown that exchangeable Ca^{2+} and Mg^{2+} occur mainly in 50:50 relationship on the surfaces of the exchanger. Hydrochemistry of the aquifer system has also been influenced by oxidation of sedimentary organic matter found in the aquifer matrix and adjacent aquitards (Pärn et al., 2018). To arrive at ^{14}C model ages, series of inverse models were developed using the inverse modelling software NETPATH (Plummer et al., 1994) and its interactive user version NETPATH-WIN (El-Kadi et al., 2011) based on the conceptual model on the geochemical evolution of groundwater described above. Specific details about the calculation of ^{14}C model ages can be found in Supplementary material (Appendix C, Table S6). The results of the inverse models together with the uncorrected ^{14}C ages and calculated ^{14}C model ages are reported in Table S3 (Supplementary material).

5. Results and discussion

5.1. Age tracers in the O-Cm aquifer system and evaluation of ^{14}C data

The results obtained for the age tracers suggest that groundwater in the O-Cm aquifer system is of considerable age (Tables S2 and S3). In only few wells near the outcrop area of the aquifer system tritium activities are above detection limit (> 0.2 TU). These measurable tritium activities were found in waters with chemical and isotopic compositions similar to modern groundwater in shallow aquifers in the study area (Pärn et al., 2016; Raidla et al., 2016). In glacial palaeogroundwater and brackish groundwater from the southern parts of the aquifer system, the tritium activities are below detection limit (< 0.2 TU). This indicates that a modern groundwater component recharged during the last 50 years is practically missing in these waters. Modern measurements of ^{3}H activities in precipitation near the northern margin of the study area in Espoo, southern Finland were in the range from 7.3 to 13.1 TU in the period 2003–2010 (IAEA/WMO, 2018). Thus, a ^{3}H activity of 0.2 TU in groundwater would indicate a fraction of modern groundwater only from 1.5 to 2.7%. ^{14}C activities of glacial palaeogroundwater in the O-Cm aquifer system are also very low, being generally < 5 pmC and yielding conventional ^{14}C ages ≥25000 ^{14}C years (Table S3).

It is well known that low radiocarbon activities measured from water cannot be directly interpreted in terms of actual groundwater

Table 2
He, Ne concentrations together with values for the Ne/He and $^3He/^4He$ ratio normalized to R_{ASW} in the studied samples from the Ordovician-Cambrian aquifer system. Excess air ($^4He_{exc}$) and radiogenic ($^4He_{rad}$) ^4He components are also given.

Well no.	Location	^4He (cc·g^{-1})	^4He error	Ne (cc·g^{-1})	Ne error	Ne/He	$^3He/^4He$ (R/R_{ASW})	$^4He_{exc}$ (cc·g^{-1})	$^4He_{rad}$ (cc·g^{-1})
Type I									
1630	Kiili*	$4.40\cdot10^{-7}$	$3.07\cdot10^{-9}$	$2.65\cdot10^{-7}$	$3.33\cdot10^{-9}$	0.60	0.25	$7.63\cdot10^{-8}$	$3.14\cdot10^{-7}$
Type II									
1551	Riisipere*	$2.35\cdot10^{-5}$	$2.92\cdot10^{-7}$	$8.57\cdot10^{-7}$	$3.24\cdot10^{-9}$	0.04	0.02	$2.47\cdot10^{-7}$	$2.33\cdot10^{-5}$
12422	Heltermaa	$3.21\cdot10^{-5}$	$3.21\cdot10^{-7}$	$8.57\cdot10^{-7}$	$4.28\cdot10^{-9}$	0.03	**	$2.47\cdot10^{-7}$	$3.18\cdot10^{-5}$
13359	Käina	$4.00\cdot10^{-5}$	$4.00\cdot10^{-7}$	$8.60\cdot10^{-7}$	$4.30\cdot10^{-9}$	0.02	**	$2.48\cdot10^{-7}$	$3.97\cdot10^{-5}$
3171	Varesmetsa	$9.22\cdot10^{-6}$	$9.22\cdot10^{-8}$	$5.09\cdot10^{-7}$	$2.57\cdot10^{-9}$	0.06	**	$1.47\cdot10^{-7}$	$9.02\cdot10^{-6}$
9483	Risti*	$2.24\cdot10^{-5}$	$2.42\cdot10^{-7}$	$8.61\cdot10^{-7}$	$2.04\cdot10^{-9}$	0.04	0.02	$2.48\cdot10^{-7}$	$2.21\cdot10^{-5}$
1562	Lehtmetsa	$3.87\cdot10^{-5}$	$3.87\cdot10^{-7}$	$8.65\cdot10^{-7}$	$4.32\cdot10^{-9}$	0.02	**	$2.49\cdot10^{-7}$	$3.84\cdot10^{-5}$
15346	Karjaküla	$1.16\cdot10^{-5}$	$1.16\cdot10^{-7}$	$8.87\cdot10^{-7}$	$4.44\cdot10^{-9}$	0.08	0.03	$2.56\cdot10^{-7}$	$1.13\cdot10^{-5}$
13305	Kõrgessaare	$9.82\cdot10^{-6}$	$9.82\cdot10^{-8}$	$1.07\cdot10^{-6}$	$5.34\cdot10^{-9}$	0.11	**	$3.07\cdot10^{-7}$	$9.46\cdot10^{-6}$
16413	Vihterpalu*	$8.57\cdot10^{-6}$	$5.73\cdot10^{-8}$	$1.10\cdot10^{-6}$	$4.07\cdot10^{-9}$	0.13	0.05	$3.16\cdot10^{-7}$	$8.20\cdot10^{-6}$
8104	Nõva*	$3.41\cdot10^{-6}$	$3.89\cdot10^{-8}$	$7.53\cdot10^{-7}$	$1.80\cdot10^{-9}$	0.22	0.04	$2.17\cdot10^{-7}$	$3.14\cdot10^{-6}$
Type III									
25755	Kose	$3.29\cdot10^{-5}$	$3.29\cdot10^{-7}$	$7.12\cdot10^{-7}$	$3.56\cdot10^{-9}$	0.02	**	$2.05\cdot10^{-7}$	$3.26\cdot10^{-5}$
11851	Võisiku	$4.72\cdot10^{-5}$	$4.72\cdot10^{-7}$	$5.36\cdot10^{-7}$	$2.68\cdot10^{-9}$	0.01	**	$1.54\cdot10^{-7}$	$4.70\cdot10^{-5}$
4002	Piilse	$1.25\cdot10^{-5}$	$1.25\cdot10^{-7}$	$7.12\cdot10^{-7}$	$3.56\cdot10^{-9}$	0.06	**	$2.05\cdot10^{-7}$	$1.22\cdot10^{-5}$
4109	Tapa	$3.18\cdot10^{-5}$	$3.18\cdot10^{-7}$	$6.01\cdot10^{-7}$	$3.01\cdot10^{-9}$	0.02	**	$1.73\cdot10^{-7}$	$3.15\cdot10^{-5}$
3508	Tamsalu	$4.02\cdot10^{-5}$	$4.02\cdot10^{-7}$	$6.90\cdot10^{-7}$	$3.45\cdot10^{-9}$	0.02	**	$1.99\cdot10^{-7}$	$4.00\cdot10^{-5}$
1679	Alu	$3.59\cdot10^{-5}$	$3.59\cdot10^{-7}$	$6.87\cdot10^{-7}$	$3.43\cdot10^{-9}$	0.02	**	$1.98\cdot10^{-7}$	$3.57\cdot10^{-5}$
5968	Estonia mine	$1.55\cdot10^{-5}$	$1.55\cdot10^{-7}$	$6.13\cdot10^{-7}$	$3.06\cdot10^{-9}$	0.04	**	$1.76\cdot10^{-7}$	$1.53\cdot10^{-5}$
Type IV									
1224	Tartu	$1.14\cdot10^{-4}$	$1.14\cdot10^{-6}$	$4.00\cdot10^{-7}$	$2.18\cdot10^{-9}$	0.00	**	$1.15\cdot10^{-7}$	$1.13\cdot10^{-4}$
3950	Värska	$1.81\cdot10^{-4}$	$1.81\cdot10^{-6}$	$4.70\cdot10^{-7}$	$2.44\cdot10^{-9}$	0.00	0.01	$1.35\cdot10^{-7}$	$1.81\cdot10^{-4}$
4471	Pärnu	$1.36\cdot10^{-4}$	$1.36\cdot10^{-6}$	$3.92\cdot10^{-7}$	$2.13\cdot10^{-9}$	0.00	0.01	$1.13\cdot10^{-7}$	$1.36\cdot10^{-4}$
8021	Häädemeeste	$2.04\cdot10^{-4}$	$2.00\cdot10^{-6}$	$4.14\cdot10^{-7}$	$1.40\cdot10^{-9}$	0.00	**	$1.19\cdot10^{-7}$	$2.04\cdot10^{-4}$
10836	Kuressaare	$5.53\cdot10^{-4}$	$5.53\cdot10^{-6}$	$6.49\cdot10^{-7}$	$3.25\cdot10^{-9}$	0.00	0.02	$1.87\cdot10^{-7}$	$5.53\cdot10^{-4}$

* He and Ne concentrations previously published in Weissbach (2014).
** No reliable ^3He result available due to very low ^3He signal in the gas split used for ^4He analysis.

age. Besides the uncertainties of initial ^{14}C activities in recharge waters and the dilution of this initial ^{14}C activity by processes discussed above (Section 4), a critical issue in ^{14}C dating concerns possible contamination of the original $a^{14}C$ signal with atmospheric ^{14}C during sampling and sample preparation. The possibility of contamination is more likely in samples collected with the conventional method where DIC is precipitated in the field as $BaCO_3$ (Gleason et al., 1969; Clark and Fritz, 1997) at a high pH (> 11) which creates a suitable environment for rapid CO_2 uptake from the atmosphere. This in turn can lead to a significant kinetic fractionation resulting in a decrease in $\delta^{13}C$ value and an increase in the ^{14}C activity of a sample (Craig, 1953; Clark and Lauriol, 1992; Aggarwal et al., 2014).

The parallel measurements by the conventional method and by the AMS method in the O-Cm aquifer system can be used to evaluate the possible ^{14}C contamination signal in groundwater. For glacial palaeogroundwater and brackish groundwater (groundwater with $\delta^{18}O$ values from −13.5 to −22.5‰), $a^{14}C$ values measured with the conventional method ranged from 1.2 to 4.4 pmC. For waters with a modern isotopic composition (groundwater with $\delta^{18}O$ values from −11.3 to −11.9‰) the $a^{14}C$ values ranged from 17.5 to 32.7 pmC. The new AMS sample taken from groundwater with a modern isotopic composition had ^{14}C activity of 29.9 pmC, which falls in the same range as samples collected with the conventional method. For glacial palaeogroundwater the AMS measurements yielded $a^{14}C$ values from 0.4 to 4.6 pmC. The ^{14}C activities in palaeogroundwater measured by the AMS were in many cases ~1 to 3 pmC lower than for samples collected by the conventional method (Table S2), which leads to a difference of about 2000–18000 ka in uncorrected ^{14}C ages. This confirmed the suspicion that some samples collected with the conventional method were subject to atmospheric CO_2 contamination. The differences between the two measurements were greater for brackish waters with higher TDS.

Nevertheless, for several wells in the north-eastern and southern parts of the study area, the $a^{14}C$ measured with the two methods were very similar (± 0.3 pmC; Table S2). Even though the exposure time to the atmosphere is greatly reduced during sampling for the AMS method, the CO_2 uptake during sampling and sample preparation cannot be excluded especially when the sampled groundwater has a high pH (> 8; Aggarwal et al., 2014). Thus, despite the correction to conventionally measured $a^{14}C$ offered by the AMS method, the $a^{14}C$ model ages calculated in this study should be considered minimum age estimates for the studied waters. In the modelling exercise, we preferably calculated ^{14}C model ages using $a^{14}C$ values measured with AMS method. For wells where the AMS and conventional measurement of $a^{14}C$ is similar, the lower value was used. Given the abovementioned uncertainties, the modelled ^{14}C ages are not calibrated and all ages including relevant background information reported in this study are given in uncalibrated ^{14}C ages BP.

5.2. Plausible models for calculating ^{14}C model ages

The models used to calculate ^{14}C model ages were evaluated based on their consistency with the measured $\delta^{13}C_{DIC}$ value in the end well (Fig. 3). Initial waters from recharge conditions that best reproduced the measured $\delta^{13}C_{DIC}$ value were considered the most plausible for calculating ^{14}C model ages (Table S3). Sensitivity analysis revealed that calculated $\delta^{13}C_{DIC}$ can vary ± 3.6‰ when either minimum and maximum values of $\delta^{13}C$ for phases is used instead of an average value (see Supplementary material, Appendix C, Table S6; Fig. 3). The ^{14}C half-life of 5730 years (Cambridge half-life) was used for age calculations (Plummer et al., 1994). The results of the modelling exercise together with the ^{14}C model ages are summarized in Table S3 (Supplementary material). The reported age is an average of model ages calculated using different initial water compositions from plausible recharge conditions.

For several samples a good correspondence between measured and calculated $\delta^{13}C_{DIC}$ values was not found with any of the initial water combinations in the chosen modelling framework (Fig. 3a). These were groundwater with the heaviest $\delta^{13}C_{DIC}$ values situated in the sulphate-reduced and methanogenic zone in the aquifer system (Pärn et al., 2018; Table S3, type "*methanogenesis*"). It was hypothesized that in addition to hydrochemical reactions described above, methanogenesis

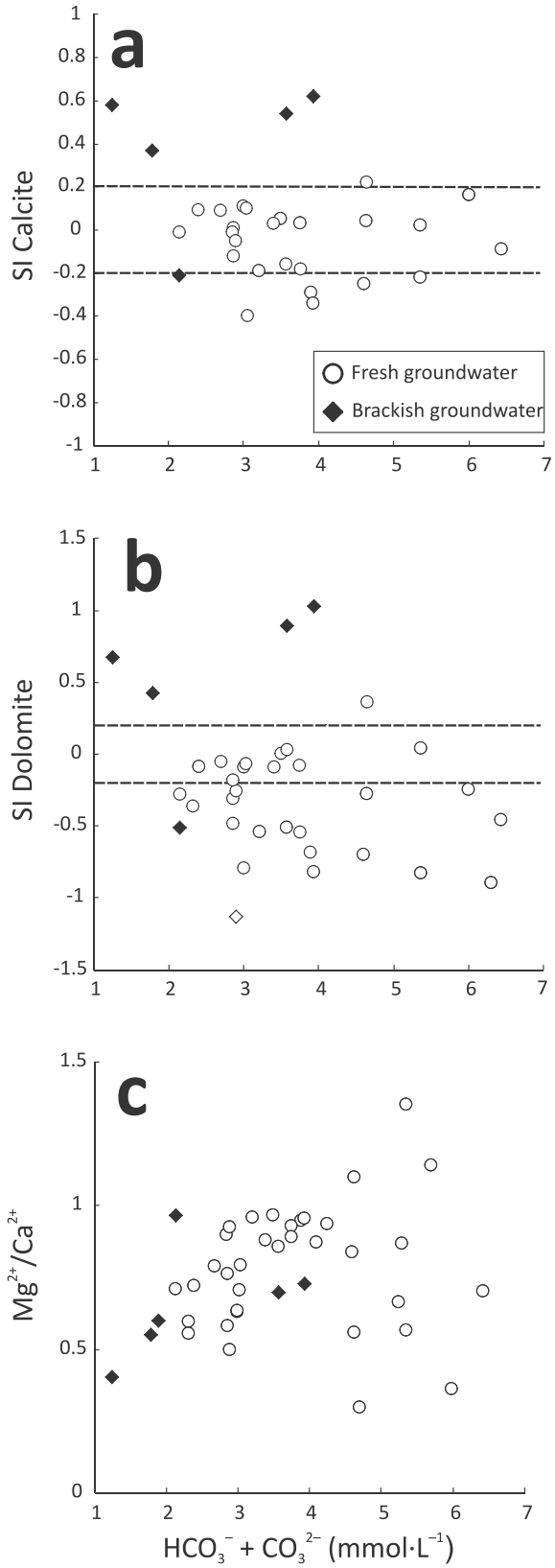

Fig. 2. The saturation indices of (a) calcite, (b) dolomite and (c) Mg^{2+}/Ca^{2+} ratios as a function of dissolved inorganic carbon ($HCO_3^- + CO_3^{2-}$) concentration in the Ordovician-Cambrian aquifer system. The area between dotted lines on (a) and (b) represents equilibrium with respect to the given mineral.

can be a relevant process influencing the $\delta^{13}C_{DIC}$ composition of these waters. During methanogenesis ^{12}C is preferentially used by bacteria and incorporated into the CH_4 molecule, while the remaining DIC becomes enriched in ^{13}C (Aravena et al., 1995a; Clark and Fritz, 1997). The magnitude of fractionation between biogenic $\delta^{13}C_{CH4}$ and parent $\delta^{13}C_{CO2}$ depends on the methanogenic pathway and is larger for carbonate reduction compared to acetate fermentation (Whiticar, 1999). Pärn et al. (2018) have shown that the isotopic composition of CH_4 in the O-Cm aquifer system is more consistent with the carbonate reduction pathway. As methane production via the acetate fermentation pathway is initially the dominant mechanism of methanogenesis in freshwater, we chose an $\varepsilon^{13}C_{CO2\text{-}CH4}$ value of 40‰ for modelling which is a value overlapped by both methanogenic pathways (Whiticar, 1999). Initial $\delta^{13}C_{CH4}$ was chosen to be −80‰ which is the most depleted value reported from the aquifer system and thus thought to be least affected by possible oxidation effects (Pärn et al., 2018). When methanogenesis is added to the processes considered by inverse modelling in NETPATH a much better correspondence between measured and calculated $\delta^{13}C_{DIC}$ values is achieved (Fig. 3b; Table S3). The remaining inconsistencies can result from uncertainties in the chosen fractionation factor and the initial $\delta^{13}C_{CH4}$ value.

5.3. ^{14}C model age of groundwater in the O-Cm aquifer system

The calculated ^{14}C model ages of groundwater in the O-Cm aquifer system were on average ~20 ka BP younger than conventional ages (Table S3) for all studied waters which shows the significance of geochemical reactions in diluting the original $a^{14}C$ activity. Based on calculated ^{14}C model ages and isotopic composition, the studied waters can be classified into four types (Types I-IV; Fig. 1) The new classification is generally in agreement with the previous classification based only on the stable isotopic composition (Pärn et al., 2016, Section 2). Groundwater with isotopic composition similar to the modern groundwater end-member ($\delta^{18}O$ from −11.3 to −11.9‰, δ^2H from −84 to −85‰) containing tritium (Type I) was characterized by negative average ^{14}C model ages within modern recharge conditions (Table S3). Negative ages can reflect the fact that the $a^{14}C$ of the last 60 years has been considerably higher than the value of 100 pmC used for atmospheric $a^{14}C$ in this study (Toth and Katz, 2006). The waters of Type I are mostly consistent with the evolution of recharge waters in both open and open/closed system conditions for calcite dissolution (see Section 4, Table 1 and Appendix B in the Supplementary material). However, previous data available from shallow groundwater in the study area do not support the occurrence of open system conditions for carbonate mineral dissolution in shallow groundwater. This would result in a measured $a^{14}C$ close to ~100 pmC which has not been observed (Table S4, Supplementary material). Instead available data suggest that groundwater with modern isotopic composition and containing tritium in the overlying shallow aquifers is characterized by $a^{14}C$ of ~40–60 pmC (Raudsep et al., 1989; Välkmann et al., 1992; Vaikmäe et al., 2001), which is characteristic of carbonate mineral dissolution in an open/closed system conditions (Table S4), where only partial isotopic exchange occurs between total inorganic carbon and soil CO_2 (van der Kemp et al., 2000). Thus, the open/closed system conditions for recharge waters are deemed more plausible for the study area.

Glacial palaeogroundwater having the most depleted isotopic composition with respect to modern groundwater ($\delta^{18}O$ from −17.7 to −22.4‰; δ^2H from −133 to −169‰) from the north-western part of the aquifer system (Type II) is consistent with closed system conditions for calcite dissolution in recharge waters from glacial conditions (Table S3). The calculated ^{14}C model ages of Type II waters range from 6 to 26 ka BP. Radiocarbon model ages younger than 11 ka BP can be judged to be affected by contamination as the ice sheet retreated from the study area ~11.3 ka BP ago (Saarse et al., 2012). Most of the Type II waters have ^{14}C model ages from ~10 to 14 ka BP which roughly coincides

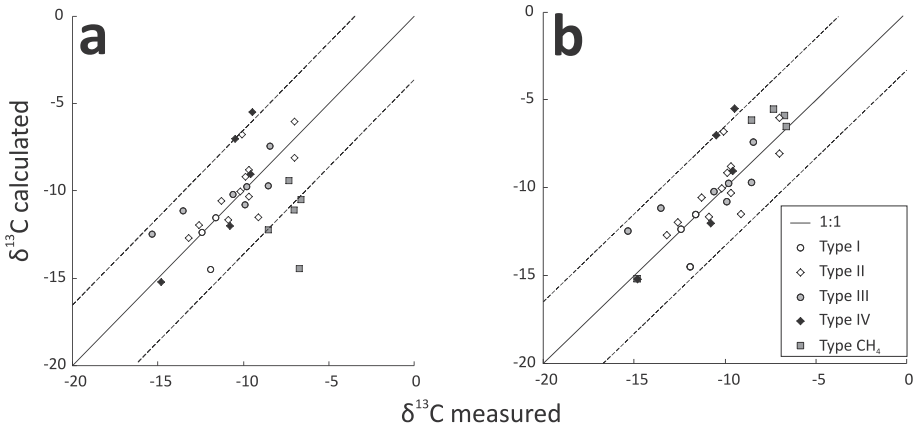

Fig. 3. Comparison between measured $\delta^{13}C$ values and $\delta^{13}C$ values calculated with NETPATH. The water types are discussed in Section 5.3. (a) $\delta^{13}C$ values calculated without methanogenesis (see text for further discussion); (b) $\delta^{13}C$ values calculated with methanogenesis (*Type CH_4*). Dashed lines show the deviation of ± 3.6‰ that can result when possible minimum or maximum estimates of the $\delta^{13}C$ value are used for phases instead of the average value (Supplementary material, Appendix C, Table S6).

with the deglaciation of the study area in the Late Glacial period (Kalm, 2006; Saarse et al., 2012). Models which describe the infiltration of glacial meltwater into aquifers (e.g. Bense and Person, 2008; Lemieux et al., 2008; McIntosh et al., 2011) suggest that most of the water did not infiltrate during the glacial maximum but during the transgression phases of continental ice sheets in the Pleistocene, when the ice sheet could not have been much thicker than 1000 m. During deglaciation of the study area, several re-advances of the ice sheet occurred. The most prominent of those was the re-advance of the Scandinavian Ice Sheet during the period from ~12.7 to 14.7 ka BP ago known as the Palivere Stage (Kalm, 2006). Palivere end-moraines related to the ice sheet re-advance are situated in the north-western part of the study area and thus coincide with the spatial distribution of Type II waters (Fig. 1). The possibility of groundwater recharge during the regression phase of the Scandinavian Ice Sheet in the Late Pleistocene is further supported by the occurrence of groundwater with the Late Glacial age in the southern parts of the BAB (Mokrik et al., 2009) and in areas near the southern and south-western margins of the BAB that were affected by glaciation during the LGM (e.g. Zuber et al., 2000; Hinsby et al., 2001).

Glacial palaeogroundwater from the north-eastern parts of the aquifer system (Type III) have calculated ^{14}C model ages ranging from ~8 to 29 ka BP. These waters have a depleted isotopic composition ($\delta^{18}O$ from −14.2‰ to −16.5‰; $\delta^{2}H$ from −104 to −131‰) with respect to modern groundwater, but their isotopic composition is heavier compared to Type II waters. Previously, it was suggested that Type III waters are a mixture between groundwater originating from glacial meltwater and modern precipitation, respectively (Pärn et al., 2016). The ^{14}C model ages calculated in this study challenge this assumption. The average age of ~17 ka BP for Type III waters coincides with the period of maximum extent of the Scandinavian Ice Sheet in the LGM rather than with the Holocene period, when the mixing with more recent meteoric waters could have occurred (Table S3). Geochemical modelling of Type III waters gave most consistent results with recharge waters evolved in open and open/closed system conditions for calcite dissolution in interstadial conditions. As discussed above, open/closed system conditions are considered more plausible for the study area. Also, open system conditions of carbonate mineral dissolution would result in even older ^{14}C model ages compared to open/closed system conditions and thus the latter provides a minimum age estimate. The calculated ^{14}C model ages suggest that the Type III waters are potentially older than Type II waters, which have a more depleted isotopic composition. This could mean that groundwater from Type III contains a component of water recharged in interstadial conditions prior to the LGM. When we assume that Type III waters have evolved through mixing between waters originating from glacial meltwater and modern precipitation, as was done previously, it would be hard to explain the greater ^{14}C model ages for Type III (mixed) waters compared to Type II (glacial) waters. So, the most plausible inference from the geochemical modelling framework adopted in this study is, that even if Type III waters have been affected by mixing with the modern meteoric end-member, they probably also contain an older component from the pre-LGM period. Results from previous studies also support the inference that Type III waters in the north-eastern part of the aquifer system could be older than Type II waters in the north-western part of the aquifer system. It has been observed that the sulphate reduction is ongoing in Type II waters, while in Type III waters it has run close to completion (Pärn et al., 2018). Also, Raidla et al. (2012) have shown that in the underlying Cambrian-Vendian aquifer system younger ^{14}C model ages characterize the western part of the aquifer system, corresponding to the regression phase of the Scandinavian Ice Sheet in the Late Pleistocene.

Brackish groundwater in deeper parts of the aquifer system (Type IV) have been shown to have ^{81}Kr ages significantly older (~550 ka) compared to the ^{14}C model ages calculated for fresh groundwater in the O-Cm aquifer system (Gerber et al., 2017). The ^{14}C model ages for Type IV waters range from ~10 to 31 ka BP with the average age of ~22 ka BP. Three of the five brackish waters dated in this study have a^{14}C model age > 25 ka BP and can be considered to lie beyond the ^{14}C dating range due to uncertainties and possible contamination effects discussed in Section 5.1. Two samples with calculated ages of 10 and 17 ka BP (wells no. 1224 and 10836) could be influenced by contamination during sampling or during sample preparation due to anomalously high a^{14}C values measured in those samples compared to other brackish waters of Type IV (Table S2). The contamination can also be connected to the leaky casing of the wells. Similarly to the palaeogroundwater of Type III, the brackish waters are also most consistent with recharge waters evolved in interstadial recharge conditions. Due to their considerable ^{81}Kr age they could also contain a meteoric component from previous interglacials (Gerber et al., 2017).

5.4. *^{4}He accumulation in the O-Cm aquifer system*

The consistency of the calculated ^{14}C model ages can be checked by studying the accumulation of radiogenic ^{4}He in groundwater. It has been observed that ^{4}He concentrations in groundwater increase with groundwater travel time (Andrews and Lee, 1979; Castro et al., 2000; Kipfer et al., 2002). He dissolved in groundwater can originate from three principle sources (Torgersen and Stute, 2013):

(a) atmospheric He in solubility equilibrium and excess air acquired during infiltration;
(b) in situ production within the aquifer matrix;
(c) He from external sources (e.g. crustal He flux).

Several lines of evidence suggest that the majority of ^{4}He in groundwater of the O-Cm aquifer system is of radiogenic origin with atmospheric and excess air components being almost negligible. The radiogenic ^{4}He component was calculated by subtracting the

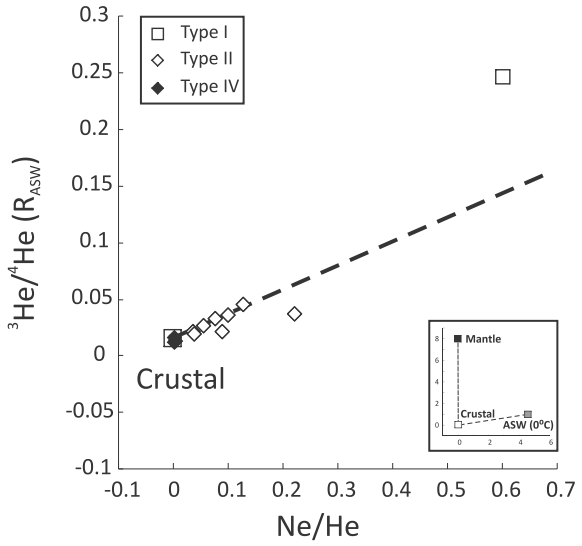

Fig. 4. The three-isotope plot of ^{3}He, ^{4}He and Ne in the Ordovician-Cambrian aquifer system. The sampled wells with available ^{3}He data are normalized to the air saturated water (ASW) ^{3}He/^{4}He ratio at 0 °C with $R_{ASW} = 1.360{\cdot}10^{-6}$ (Benson and Krause, 1980). In addition to air saturated water at 0 °C (ASW with normalized ^{3}He/^{4}He ratio of 1 and Ne/He ratio of 4.59; grey square), the crustal end-member (normalized ^{3}He/^{4}He ratio of 0.0153 and Ne/He ratio of 0, Mamyrin and Tolstikhin (1984); white square) and the mantle end-member (normalized ^{3}He/^{4}He ratio of 8 and Ne/He of 0, Graham (2002); black square) are also depicted. The dashed lines indicate the mixing lines between the end-members. The size of the symbols is larger than the analytical precision for both ratios.

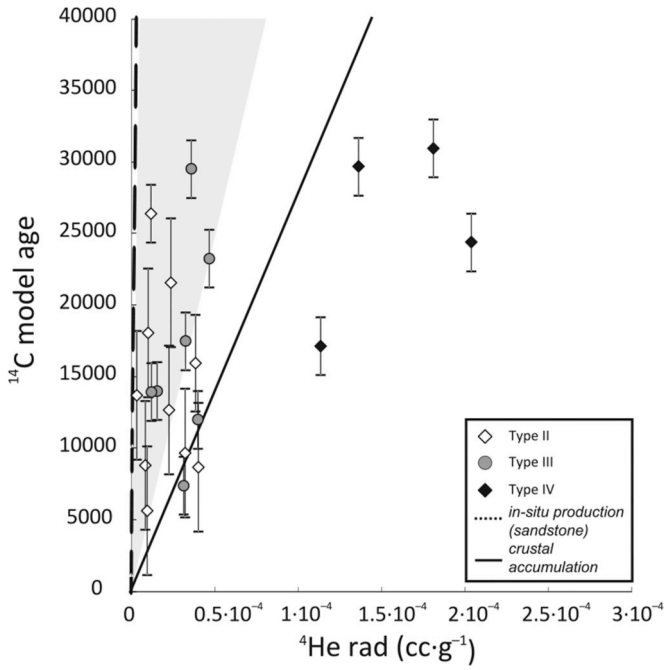

Fig. 5. Modelled ^{14}C ages as a function of radiogenic ^{4}He in the Ordovician-Cambrian aquifer system. The dashed line shows the in-situ production rate in Cambrian and Lower Ordovician sandstone. The grey area between the two solid lines shows the range for the maximum ^{4}He accumulation rate calculated based on the parameters given in Table 3. The error bars for ^{14}C model ages reflect the standard deviation of ages derived from acceptable models for each sample (Table S3, Supplementary material). The accumulation of He from an external flux in cm^3 (STP) cm^{-3}a^{-1} is calculated from the continental degassing flux of $3.4{\cdot}10^{-6}$ cm^3 (STP) cm^{-2}a^{-1} (Oxburgh and O'Nions, 1987), the average thickness of the aquifer system of 60 m and the average porosity of 0.2.

equilibrium concentration of ^{4}He in air-saturated water at 0 °C and the excess air component from the total ^{4}He concentrations. The excess air component was estimated using the Ne concentrations (Table 2). Most samples contain substantial excesses of Ne above equilibrium, indicating the presence of an excess air component, which for ^{4}He is estimated according to Torgersen and Stute (2013, Eq. 8.5), assuming an atmospheric He/Ne ratio of this component. It must be noted that complete noble gas datasets from glacial palaeogroundwater of the BAB (e.g. Weissbach, 2014) show highly unusual excess air patterns, where Ne is strongly depleted with respect to excess air amounts predicted by the usual excess air models (Weissbach, 2014; Raidla et al., 2017). As this depletion may also affect excess air of He, the applied estimate for the excess air component is likely to be a maximum estimate, leading to a minimum estimate for radiogenic He. However, the effects are very small, as radiogenic He dominates in all samples (Table 2).

Relations between normalized ^{3}He/^{4}He ratio and total concentrations of He and Ne (Fig. 4) confirm this inference as all samples with available ^{3}He data plot very close to the crustal end-member indicating that ^{4}He in studied waters is almost solely of radiogenic origin. The samples with missing ^{3}He results would probably also have a very low radiogenic ^{3}He/^{4}He ratio, since ^{3}He signals were too low for a reliable measurement. The brackish waters (Type IV) plot almost on the crustal end-member values. Type II samples plot on the mixing line with the atmospheric end-member, whereas the single Type I sample plots above the line, possibly due to tritiogenic ^{3}He in this relatively young sample, which contains about 5 TU of tritium (Weissbach, 2014).

In general, the calculated radiogenic ^{4}He concentrations seem to support the assumptions on relative age differences between different water types that were based on calculated ^{14}C model ages (Fig. 5). The in-situ ^{4}He accumulation rate (A_{He}; cm^{3}STPcm^{-3}a^{-1}) can be calculated based on the U and Th concentrations in the aquifer-forming minerals (Castro et al., 2000; Wen et al., 2016):

$$A_{He} = (1.207{\cdot}10^{-13} \times C_U + 2.867{\cdot}10^{-14} \times C_{Th}) \times \rho_r \times \Lambda_{He} \times \frac{1-n}{n} \quad (1)$$

where Λ_{He} is the release factor of He from minerals to water (usually taken to be 1; Torgersen and Stute, 2013), C_U and C_{Th} are the average concentrations of U and Th in ppm; ρ_r is the average density and n is porosity of the reservoir rock, respectively. The overview of parameters used in the calculation of A_{He} and the calculated A_{He} for geological strata associated with the aquifer system are given in Table 3. The in-situ production of the sandstone in the aquifer matrix is small (average $5.5{\cdot}10^{-11}$ cm^{3}STPcm^{-3}a^{-1}; Table 3) and yields ^{4}He accumulation rates markedly smaller than suggested by ^{14}C model ages (Fig. 5). However, the Lower Ordovician black shale that is in contact with the upper part of the Cambrian and Lower Ordovician sandstones is notable for its high U concentrations (average concentrations in western and eastern Estonia are 88 and 236 ppm, respectively, Petersell, 1997; Voolma et al., 2013; Hade and Soesoo, 2014). Thus, it can be proposed that the real ^{4}He accumulation rate in the aquifer system is much larger than the in-situ production rate calculated from U concentrations in the sandstones. When the contribution to ^{4}He accumulation rate from the shale and the clay are also taken into account, the estimated maximum ^{4}He accumulation rates increase to values from $1.2{\cdot}10^{-10}$ to $2.0{\cdot}10^{-9}$ cm^{3}STPcm^{-3}a^{-1}, respectively, depending on the values of parameters used (Table 3; Fig. 5).

The measured radiogenic He concentrations generally increase with increasing ^{14}C model ages (Fig. 5). However, despite a general agreement with radiogenic He isotope concentrations and calculated ^{14}C model ages, the ^{4}He accumulation rates suggest that in many cases the groundwater ages are older compared to ^{14}C model ages calculated for glacial palaeogroundwater (Types II and III). Furthermore, brackish groundwater of Type IV plot above the area defined by calculated ^{4}He accumulation rates and close to the crustal degassing flux of ^{4}He (Oxburgh and O'Nions, 1987; Fig. 5). A possible explanation of this relation is that the calculated ^{14}C model ages presented in this study

Table 3
Parameters in Eq. (1) and the calculated A_{He} for geological strata associated with the Ordovician-Cambrian aquifer system.

Hydrogeological unit	C_U	C_{Th}	p_r	p_w	n	A_{He}	Publications
	ppm		*g cm^{-3}*	*g cm^{-3}*		*cm^{3}STP g^{-1} a^{-1}*	
Ordovician-Cambrian aquifer system: sandstone - *minimum estimate*	38	–	2.6	1	0.3	$2.8{\cdot}10^{-11}$	Raudsep (1997)
Ordovician-Cambrian aquifer system: sandstone - *maximum estimate*	50	–	2.6	1	0.15	$8.9{\cdot}10^{-11}$	Raudsep (1997)
Lower Ordovician graptolite argillite - *minimum estimate*	88	14	1.8	1	0.2	$9.1{\cdot}10^{-11}$	Croff et al. (1985); Petersell (1997) Voolma et al. (2013); Soesoo & Hade (2014)
Lower Ordovician graptolite argillite - *maximum estimate*	236	14	1.8	1	0.05	$1.9{\cdot}10^{-9}$	Croff et al. (1985); Petersell (1997) Voolma et al. (2013); Soesoo & Hade (2014)
Lükati-Lontova aquitard: claystone - *minimum estimate*	3.6	12.4	2.2	1	0.15	$9.1{\cdot}10^{-11}$	Kiipli et al. (2000)
Lükati-Lontova aquitard: claystone - *maximum estimate*	3.6	12.4	2.2	1	0.25	$4.3{\cdot}10^{-10}$	Kiipli et al. (2000)
Total (*minimum estimate)*						**$1.2{\cdot}10^{-10}$**	
Total (*maximum estimate)*						**$2.0{\cdot}10^{-9}$**	

need to be considered minimal ages due to various contamination effects that could modify the measured a^{14}C value (Section 5.1). This assumption is supported by much larger ^{81}Kr ages estimated for brackish groundwater (~550 ka BP; Gerber et al., 2017). However, these inferences are complicated by the fact that the concentration of radiogenic ^{4}He in groundwater from the O-Cm aquifer system can be influenced by mixing between glacial palaeogroundwater and much older saline formation water (Pärn et al., 2016; Gerber et al., 2017). Thus, the high ^{4}He concentrations in studied groundwater are probably also related to mixing between very old water with a very high He concentrations and younger water of low salinity and lower He concentrations (cf. Lehmann et al., 1996).

5.5. Groundwater age distribution in the Ordovician-Cambrian aquifer system

Strong influence of mixing between groundwater of different origin (modern recharge, glacial meltwater from the Pleistocene, saline formation water and brine) has probably resulted in wide age distributions in the studied waters. This can be illustrated by relations between radiogenic ^{4}He, δ^{18}O values and Cl^- concentrations (Fig. 6a and b). Glacial palaeogroundwater with the lightest isotope composition of Type II from the north-western part of the study area has the lowest radiogenic ^{4}He content and the latter increases with enrichment in δ^{18}O values (Fig. 6a). This indicates increasing groundwater residence times and mixing with older groundwater from the deeper parts of the aquifer system. The same general pattern as in Type II waters is visible in Type III waters with higher concentrations of radiogenic ^{4}He corresponding to heavier δ^{18}O values. This supports the assumption that glacial palaeogroundwater with most depleted isotopic composition could indeed represent waters originating from the latest advance of the Scandinavian Ice Sheet during the Palivere stage from ~14.7 to 12.7 ka BP (Kalm, 2006). Waters with higher radiogenic ^{4}He content could contain a more important fraction of groundwater from the pre-LGM period.

However, the relations in Fig. 6a and b suggest that mixing processes have been markedly different for brackish groundwater of Type IV compared to glacial palaeogroundwater of Type II and III. Brackish groundwater of Type IV has radiogenic ^{4}He contents of a magnitude higher compared to glacial palaeogroundwater in line with much older ^{81}Kr ages estimated by Gerber et al. (2017). Previous studies (Pärn et al., 2016, 2018; Gerber et al., 2017) have shown that Type IV groundwater is a mixture of groundwater with glacial origin, a meteoric component possibly originating from previous interglacials and brine in the central parts of the basin. This is supported by the relation between Cl^- and radiogenic ^{4}He (Fig. 6b), which shows that the majority of ^{4}He in the studied waters has been acquired by mixing with the saline formation water and brine from the deeper parts of the basin. Thus, Type IV groundwater certainly contains much older components with respect to glacial palaeogroundwater (Types II and III) as suggested by radiogenic ^{4}He concentrations. This older component has been related to Na-Cl type brines in the central parts of the BAB which have ^{81}Kr ages beyond the ^{81}Kr dating range (> 1.3 Ma; Gerber et al., 2017). As halite is not present in the aquifer matrix, the high chloride concentrations found in the brine suggest, that they have most likely evolved from evaporated seawater later modified by water-rock interaction (Pärn et al., 2016; Gerber et al., 2017). Furthermore, values of the Li^+/Cl^-, Na^+/Cl^- and Br^-/Cl^- ratios are similar to seawater in both Type IV groundwater in the O-Cm aquifer system and in the brine (Pärn et al., 2016; Gerber et al., 2017). Thus, the brine component is potentially very old and probably of pre-Quaternary origin (Mokrik, 1997; Gerber et al., 2017).

In previous studies (e.g. Aquilina et al., 2015; Aquilina and de Dreuzy, 2011), diffusion has been reported as the main process for the source of solutes in saline groundwater with long residence time. Several lines of evidence suggest that dispersive mixing rather than diffusion has been the main process that has led to the development of a wide age distribution and the observed salinity gradient (chloride concentrations) in the O-Cm aquifer system. Firstly, Type IV

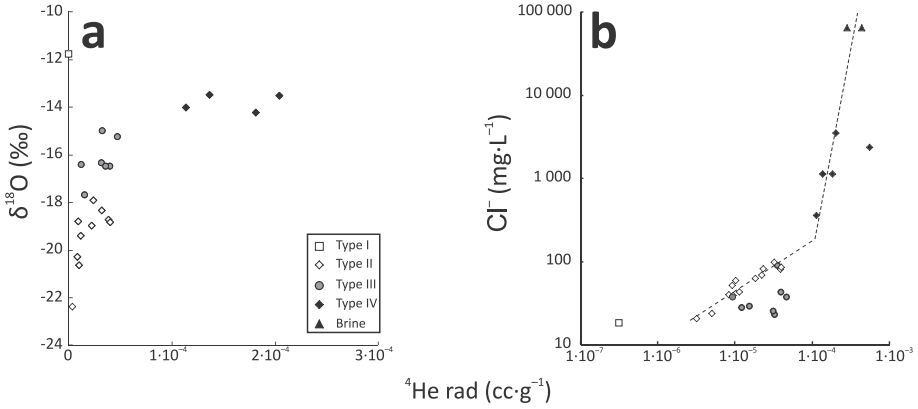

Fig. 6. (a) δ^{18}O composition and (b) Cl^- concentrations of groundwater as a function of radiogenic ^{4}He in the Ordovician-Cambrian aquifer system. For a clearer representation of the majority of the samples, the Kuressaare sample with the highest radiogenic ^{4}He concentration (Table 2) is omitted from the figure (a). The samples representing the brine endmembers in figure (b) are located in the Riga area, Latvia and the data is reported in Gerber et al. (2017). The dashed lines in figure (b) are fit through data to show hypothetical mixing lines between brine and waters of Type IV and between Type II and Type IV waters.

groundwater has an isotopic composition markedly lighter ($\delta^{18}O$ from −13.5 to −17.3‰) compared to the brine ($\delta^{18}O$ value of ~ −4.5‰; Babre et al., 2016; Gerber et al., 2017), which can be explained by mixing with glacial palaeogroundwater. Secondly, Gerber et al. (2017) have shown that the patterns of ^{81}Kr ages together with radiogenic ^{4}He and ^{40}Ar in groundwater of Type IV and brine cannot be explained by assuming that the deep groundwater has been almost stagnant on time scales of several hundred thousand years. The same point is also highlighted by calculating the diffusion length scale from $\sqrt{\theta \cdot D_m \cdot t}$ (θ – effective porosity; D_m – molecular diffusion of water molecules in water; t – times since recharge) for sample no. 8021 (Table 2; Appelo and Postma, 2005; Aquilina et al., 2015). From this sample an ^{81}Kr age of 541 ± 28 ka has been reported (Gerber et al., 2017). If the effective porosity in the range of 0.05–0.2 is assumed (Gerber et al., 2017), the resulting diffusion length scale would be only 30–50 m. At the same time, the chemical and isotopic composition of Type IV waters is markedly different from brines which lie approximately 150 km to the south.

Thus, due to the mixing processes described above, the studied samples seem to contain fractions of water with strongly differing ages. It should be kept in mind, that while the ^{14}C model ages (and also ^{81}Kr ages) date the meteoric component (precipitation, glacial meltwater) of groundwater, the radiogenic ^{4}He component mostly depends on mixing with older saline groundwater (cf. Gerber et al., 2017). The observed discrepancies in age estimates provided by different age tracers can be explained by assuming that in the shallower northern part of the aquifer system significant changes in groundwater composition can be brought about by glacial meltwater intrusion during a single glaciation. At the same time, multiple glacial-interglacial cycles are needed to transport the glacial meltwater signature to the deeper southern parts of the aquifer system. Indeed, the numerical modelling carried out by Sterckx et al. (2018) has shown that glacial meltwater did not infiltrate to distances greater than 175 km in the northern part of the BAB during the LGM. At the same time groundwater of Type IV lies approximately 200–250 km to the south from the outcrop area of the aquifer system. This supports the inference, drawn based on ^{14}C model ages and radiogenic ^{4}He concentrations, that groundwater originating from previous glacial-interglacial cycles is present in the O-Cm aquifer system (Sections 5.3-5.4; Gerber et al., 2017). Furthermore, this would also mean that glacial palaeogroundwater originating from the LGM period would not have mixed with the brine in the central parts of the basin (cf. Raidla et al., 2009; Pärn et al., 2016), but rather with brackish groundwater of Type IV which was already a product of mixing between glacial meltwater and saline formation water from the previous glacial-interglacial cycles.

Finally, Raidla et al. (2012) dated the glacial palaeogroundwater from the underlying Cambrian-Vendian aquifer system to the period from 14 to 27 ka BP and deemed it to be coeval with the advance and maximum extent of the Scandinavian Ice Sheet in the LGM. In the light of the results provided here, it should be considered whether there is evidence for the presence of groundwater originating from previous interstadials and glacial-interglacial cycles in the Cambrian-Vendian aquifer system. This could be possible as the Cambrian-Vendian aquifer system is much better protected from mixing with modern groundwater from shallow aquifers than the overlying O-Cm aquifer system.

6. Conclusion

Despite the shortcomings discussed above, the first attempt to date the palaeogroundwater in the O-Cm aquifer system allowed us to identify groundwater originating from three different climatic periods: (1) the post-glacial period (0–12 ka BP); (2) the LGM (~12–22 ka BP) and (3) the pre-LGM period (> 22 ka BP). Part of the glacial palaeogroundwater in the northern part of the aquifer system is consistent with dissolution of calcite in open/closed system conditions which is a more likely scenario for interstadial time periods when the Scandinavian Ice Sheet did not reach the study area. Glacial palaeogroundwater situated in the north-western parts of the study area is consistent with closed system dissolution of calcite which points to the direct origin from glacial meltwater recharge. Future studies should consider whether this difference in ^{14}C model ages between two parts of the aquifer system is caused by a prominent movement of the Scandinavian Ice Sheet from west to east or by secondary effects (e.g. choices made in modelling, modification of initial ^{14}C signal by contamination). As ^{14}C model ages for several samples of glacial palaeogroundwater in the aquifer system are ≥20 ka BP, age tracers having longer half-lives (e.g. ^{81}Kr) should be used in future studies to better constrain the groundwater age distribution.

Comparison between ^{14}C model ages and ^{4}He accumulation rates showed that groundwater ages based on ^{4}He accumulation would be systematically older. However, the ^{4}He in the majority of studied waters seems to be acquired through mixing with very old saline formation water and brine from the deep parts of the basin which complicates the calculation of ^{4}He accumulation ages. Thus, groundwater in the O-Cm aquifer system probably has a wide age distribution containing fractions of water with markedly different ages. The observed pattern of ^{14}C model ages, radiogenic ^{4}He concentrations and previously published ^{81}Kr ages suggest that the aquifer system probably also contains groundwater originating from pre-LGM period. Such results complement the inferences drawn by Gerber et al. (2017) for the deep part of the BAB, by showing that groundwater originating from pre-LGM period is already present in shallower northern parts of the deepest sedimentary aquifers in the BAB. This offers further support to the hypothesis that these deep aquifers must have been in a transient state for large parts of the Pleistocene (Gerber et al., 2017).

Acknowledgements

The activities of the present study were supported by the Estonian Research Council Project IUT19-22 (R.V.), PUTJD127 (V.R.) and Archimedes Foundation Kristjan Jaak Scholarship no. 16-3.5/948 (J.P.). The paper is a contribution to the INQUA/UNESCO supported G@GPS Project. The authors would like to thank Heivi Rajamäe for the ^{14}C sample preparation at Department of Geology, Tallinn University of Technology and Hannes Martma for assistance during stable isotope measurements at Department of Geology, Tallinn University of Technology. The main author would also like to thank Christoph Gerber from CSIRO, Australia for fruitful discussions and constructive comments that helped to improve the manuscript. Finally, we would like to thank Michael Fletcher from the Geological Survey of Estonia for editing the manuscript for English. The paper was improved significantly by the constructive comments of two anonymous reviewers.

Appendix. Supplementary material

Supplementary material to this article can be found online at https://doi.org/10.1016/j.apgeochem.2019.01.004.

References

Aeschbach-Hertig, W., Solomon, D.K., 2013. Noble gas thermometry in groundwater hydrology. In: Burnard, P. (Ed.), The Noble Gases as Geochemical Tracers. Springer Verlag, pp. 81–122.

Aeschbach-Hertig, W., Stute, M., Clark, J.F., Reuter, R.F., Schlosser, P., 2002. A paleotemperature record derived from dissolved noble gases in groundwater of the Aquia Aquifer (Maryland, USA). Geochem. Cosmochim. Acta 66, 797–817. https://doi.org/10.1016/S0016-7037(01)00804-3.

Aggarwal, P.K., Araguas-Araguas, L., Choudhry, M., van Duren, M., Froehlich, K., 2014. Lower groundwater ^{14}C age by atmospheric CO_2 uptake during sampling and analysis. Gr. Water 52, 20–24. https://doi.org/10.1111/gwat.12110.

Andrews, J.N., Lee, D.J., 1979. Inert gases in groundwater from the Bunter Sandstone of England as indicators of age and palaeoclimatic trends. J. Hydrol 41, 233–252. https://doi.org/10.1016/0022-1694(79)90064-7.

Appelo, C.A.J., Postma, D., 2005. Geochemistry, groundwater and pollution, second ed. Balkema, Leiden, The Netherlands.

Aquilina, L., de Dreuzy, J.-R., 2011. Relationship of present saline fluid with paleomigration of basinal brines at the basement/sediment interface (Southeast basin – France). Appl. Geochem. 26, 1933–1945.
Aquilina, L., Vergnaud-Ayrauld, V., Armandine les Landes, A., Pauwels, H., Davy, P., Petelet-Giraud, E., Labasque, T., Roques, C., Chatton, E., Bour, O., Ben Maamar, S., Dufresne, A., Khaska, M., Le Gal La Salle, A., Barbecot, F., 2015. Impact of climate changes during the last 5 million years on groundwaters in basement aquifers. Sci. Rep. 5, 14132. https://doi.org/10.1038/srep14132. https://doi.org/10.1038/srep14132.
Aravena, R., Wassenaar, L.I., Barker, J.F., 1995a. Distribution and isotopic characterization of methane in a confined aquifer in southern Ontario, Canada. J. Hydrol 173, 51–70.
Aravena, R., Wassenaar, L.I., Plummer, N.L., Barker, J.F., 1995b. Estimating ^{14}C groundwater ages in a methanogenic aquifer. Water Resour. Res. 31, 2307–2317.
Babre, A., Kalvāns, A., Popovs, K., Retiķe, I., Dēliņa, A., Vaikmäe, R., Martma, T., 2016. Pleistocene age paleo-groundwater inferred from water-stable isotope values in the central part of the Baltic Artesian Basin. Isot. Environ. Health Stud. 52, 706–725. https://doi.org/10.1080/10256016.2016.1168411.
Bense, V.F., Person, M.A., 2008. Transient hydrodynamics within intercratonic sedimentary basins during glacial cycles. J. Geophys. Res. 113, F04005. https://doi.org/10.1029/2007JF000969.
Benson, B.B., Krause, D., 1980. Isotopic fractionation of helium during solution: A probe for the liquid state. J. Solut. Chem. 9, 895–909. https://doi.org/10.1007/BF00646402.
Blaser, P.C., Coetsiers, M., Aeschbach-Hertig, W., Kipfer, R., Van Camp, M., Loosli, H.H., Walraevens, K., 2010. A new groundwater radiocarbon correction approach accounting for palaeoclimate conditions during recharge and hydrochemical evolution: The Ledo-Paniselian Aquifer, Belgium. Appl. Geochem. 25, 437–455. https://doi.org/10.1016/j.apgeochem.2009.12.011.
Boulton, G.S., Caban, P., van Gijssel, K., 1995. Groundwater flow beneath ice sheets: Part I – Large scale patterns. Quat. Sci. Rev. 14, 545–562.
Brand, W., Heike, G., C.E., R., R.C., W., 2009. Cavity ring-down spectroscopy versus high-temperature conversion isotope ratio mass spectrometry; a case study on δ^2H and $\delta^{18}O$ of pure water samples and alcohol/water mixtures. Rapid Commun. Mass Spectrom. 23, 1879–1884. https://doi.org/10.1002/rcm.4083.
Castro, M.C., Stute, M., Schlosser, P., 2000. Comparison of ^4He ages and ^{14}C ages in simple aquifer systems: Implications for groundwater flow and chronologies. Appl. Geochem. 15, 1137–1167. https://doi.org/10.1016/S0883-2927(99)00113-4.
Cendón, D.I., Hankin, S.I., Williams, J.P., Van der Ley, M., Peterson, M., Hughes, C.E., Meredith, K., Graham, I.T., Hollins, S.E., Levchenko, V., Chisari, R., 2014. Groundwater residence time in a dissected and weathered sandstone plateau: Kulnura-Mangrove Mountain aquifer, NSW, Australia. Aust. J. Earth Sci. 61, 475–499. https://doi.org/10.1080/08120099.2014.893628.
Clark, I.D., Fritz, P., 1997. Environmental Isotopes in Hydrogeology. CRC Press, New York.
Clark, I.D., Lauriol, B., 1992. Kinetic enrichment of stable isotopes in cryogenic calcites. Chem. Geol. 102, 217–228. https://doi.org/10.1016/0009-2541(92)90157-Z.
Cloutier, V., Lefebvre, R., Savard, M.M., Therrien, 2010. Desalination of a sedimentary rock aquifer system invaded by Pleistocene Champlain Sea water and processes controlling groundwater geochemistry. Environ. Earth Sci. 59 977–944.
Coetsiers, M., Walraevens, K., 2009. A new correction model for ^{14}C ages in aquifers with complex geochemistry - Application to the Neogene Aquifer, Belgium. Appl. Geochem. 24, 768–776. https://doi.org/10.1016/j.apgeochem.2009.01.003.
Corcho Alvarado, J.A., Purtschert, R., Barbecot, F., Chabault, C., Rueedi, J., Schneider, V., Aeschbach-Hertig, W., Kipfer, R., Loosli, H.H., 2007. Constraining the age distribution of highly mixed groundwater using ^{39}Ar: A multiple environmental tracer ($^3H/^3He$, ^{85}Kr, ^{39}Ar, and ^{14}C) study in the semiconfined Fontainebleau Sands Aquifer (France). Water Resour. Res. 43, W03427. https://doi.org/10.1029/2006WR005096.
Craig, H., 1953. The geochemistry of the stable carbon isotopes. Geochem. Cosmochim. Acta 3, 53–92. https://doi.org/10.1016/0016-7037(53)90001-5.
Croff, A.G., Lomenick, T.F., Lowrie, R.S., Stow, S.H., 1985. Evaluation of five sedimentary rocks other than salt for high level waste repository siting purposes. Oak Ridge Nat. Lab. ORNL/CF-85/2/V2. Oak Ridge, Tennessee.
El-Kadi, A.I., Plummer, L.N., Aggarwal, P., 2011. NETPATH-WIN: An interactive user version of the mass-balance model, NETPATH. Gr. Water 49, 593–599. https://doi.org/10.1111/j.1745-6584.2010.00779.x.
Ferguson, G.A.G., Betcher, R.N., Grasby, S.E., 2007. Hydrogeology of the Winnipeg formation in Manitoba, Canada. Hydrogeol. J. 15, 573–587.
Fontes, J.-C., 1981. Palaeowaters. In: Gat, J.R., Gonfiantini, R. (Eds.), Stable Isotope Hydrology. Deuterium and Oxygen-18 in the Water Cycle. IAEA, Vienna, pp. 273–298.
Fontes, J.-C., Garnier, J.-M., 1979. Determination of the initial ^{14}C activity of the total dissolved carbon: A review of the existing models and a new approach. Water Resour. Res. 15, 399–413. https://doi.org/10.1029/WR015i002p00399.
Gerber, C., Vaikmäe, R., Aeschbach, W., Babre, A., Jiang, W., Leuenberger, M., Lu, Z.T., Mokrik, R., Müller, P., Raidla, V., Saks, T., Waber, H.N., Weissbach, T., Zappala, J.C., Purtschert, R., 2017. Using ^{81}Kr and noble gases to characterize and date groundwater and brines in the Baltic Artesian Basin on the one-million-year timescale. Geochem. Cosmochim. Acta 205, 187–210. https://doi.org/10.1016/j.gca.2017.01.033.
Geyh, M., 2000. Groundwater. Saturated and Unsaturated Zone. Technical Documents in Hydrology No. vol. 39, vol. IV UNESCO, Paris.
Gleason, J.D., Friedman, I., Hanshaw, B.B., 1969. Extraction of dissolved carbonate species from natural water for carbon-isotope analysis. U.S. Geological Survey Professional Paper 650-D D248–D250.
Gleeson, T., Van der Steen, J., Sophocleous, M.A., Taniguchi, M., Alley, W.M., Allen, D.M., Zhou, Y., 2010. Groundwater sustainability strategies. Nat. Geosci. 3, 378–379. https://doi.org/10.1038/ngeo881.
Gleeson, T., Befus, K.M., Jasechko, S., Luijendijk, E., Cardenas, M.B., 2016. The global volume and distribution of modern groundwater. Nat. Geosci. 9, 161–164. https://doi.org/10.1038/ngeo2590.
Graham, D.W., 2002. Noble Gas Isotope Geochemistry of Mid-Ocean Ridge and Ocean Island Basalts: Characterization of Mantle Source Reservoirs. Rev. Mineral. Geochem. 47, 247–317. https://doi.org/10.2138/rmg.2002.47.8.
Grasby, S.E., Osadetz, K., Betcher, R., Render, F., 2000. Reversal of the regional-scale flow system of the Williston Basin in response to Pleistocene glaciation. Geology 29, 635–638.
Grundl, T., Magnusson, N., Brennwald, M.S., Kipfer, R., 2013. Mechanisms of subglacial groundwater recharge as derived from noble gas, ^{14}C, and stable isotopic data. Earth Planet. Sci. Lett. 369–370, 78–85. https://doi.org/10.1016/j.epsl.2013.03.012.
Hade, S., Soesoo, A., 2014. Estonian graptolite argillites revisited: A future resource? Oil Shale 31, 4–18. https://doi.org/10.3176/oil.2014.1.02.
Han, L.-F., Plummer, L.N., 2013. Revision of Fontes & Garnier's model for the initial ^{14}C content of dissolved inorganic carbon used in groundwater dating. Chem. Geol. 351, 105–114.
Hinsby, K., Harrar, W.G., Nyegaard, P., Konradi, P.B., Rasmussen, E.S., Bidstrup, T., Gregersen, U., Boaretto, E., 2001. The Ribe Formation in western Denmark - Holocene and Pleistocene groundwaters in a coastal Miocene sand aquifer. In: In: Edmunds, W.M., Milne, C.J. (Eds.), Palaeowaters of Coastal Europe: Evolution of Groundwater since the late Pleistocene, vol. 189. Geological Society, Special Publications, London, pp. 29–44.
IAEA, WMO, 2018. WISER – Water Isotope System for data analysis, visualization and Electronic Retrieval. 4.29.18. https://nucleus.iaea.org/wiser/index.aspx.
Jasechko, S., Perrone, D., Befus, K.M., Bayani Cardenas, M., Ferguson, G., Gleeson, T., Luijendijk, E., McDonnell, J.J., Taylor, R.G., Wada, Y., Kirchner, J.W., 2017. Global aquifers dominated by fossil groundwaters but wells vulnerable to modern contamination. Nat. Geosci. 10, 425–429. https://doi.org/10.1038/ngeo2943.
Juodkazis, V. (Ed.), 1980. Hydrogeological Map of the Pre-quaternary Deposits of the Soviet Baltic Republics. Ministry of Geology of the USSR.
Kalin, R.M., 2000. Radiocarbon Dating of Groundwater Systems. In: Environmental Tracers in Subsurface Hydrology, . https://doi.org/10.1007/978-1-4615-4557-6_4.
Kalm, V., 2006. Pleistocene chronostratigraphy in Estonia, southeastern sector of the Scandinavian glaciation. Quat. Sci. Rev. 25, 960–975. https://doi.org/10.1016/j.quascirev.2005.08.005.
Kiipli, T., Batchelor, R.A., Bernal, J.P., Cowing, C., Hagel-Brunnstrom, M., Ingham, M.N., Johnson, D., Kivisilla, J., Knaack, C., Kump, P., Lozano, R., Michiels, D., Orlova, K., Pirrus, E., Rousseau, R.M., Ruzicka, J., Sandstrom, H., Willis, J.P., 2000. Seven sedimentary rock reference samples from Estonia. Oil Shale 17, 215–223.
Kipfer, R., Aeschbach-Hertig, W., Peeters, F., Stute, M., 2002. Noble Gases in Lakes and Ground Waters. Rev. Mineral. Geochem. 47, 615–700. https://doi.org/10.2138/rmg.2002.47.14.
Kreuzer, A., 2007. Paläotemperaturstudie mit Edelgasen im Grundwasser der Nordchinesischen Tiefebene. PhD thesis. Ruprecht-Karls-Universität, Heidelberg.
Lehmann, B.E., Loosli, H.H., Purtschert, R., Andrews, J.N., 1996. A comparison of chloride and helium concentrations in deep groundwaters. In: Isotopes in water resources management,, vol. 1. IAEA, Vienna, pp. 3–17.
Lemieux, J.M., Sudicky, E.A., Peltier, W.R., Tarasov, L., 2008. Dynamics of groundwater recharge and seepage over the Canadian landscape during Wisconsinian glaciation. J. Geophys. Res. 113, F01011. https://doi.org/10.1029/2007JF000838.
Mamyrin, B.A., Tolstikhin, I.N., 1984. Helium Isotopes in Nature, vol. 3 Elsevier, Amsterdam, New York, Tokyo.
McCallum, J.L., Cook, P.G., Simmons, C.T., Werner, A.D., 2014. Bias of apparent tracer ages in heterogeneous environments. Gr. Water 52, 239–250. https://doi.org/10.1111/gwat.12052.
McIntosh, J.C., Walter, L.M., 2006. Paleowaters in Silurian–Devonian carbonate aquifers: geochemical evolution of groundwater in the Great Lakes region since the Late Pleistocene. Geochem. Cosmochim. Acta 70, 2454–2479.
McIntosh, J.C., Garven, G., Hanor, J.S., 2011. Impacts of Pleistocene glaciation on large-scale groundwater flow and salinity in the Michigan Basin. Geofluids 11, 18–33.
Mokrik, R., Mažeika, J., Baublyte, A., Martma, T., 2009. The groundwater age in the Middle-Upper Devonian aquifer system, Lithuania. Hydrogeol. J. 17, 871–889. https://doi.org/10.1007/s10040-008-0403-1.
Oxburgh, E.R., O'Nions, R.K., 1987. Helium Loss, Tectonics, and the Terrestrial Heat Budget. Science 237, 1583–1588. https://doi.org/10.1126/science.237.4822.1583.
Pärn, J., Raidla, V., Vaikmäe, R., Martma, T., Ivask, J., Mokrik, R., Erg, K., 2016. The recharge of glacial meltwater and its influence on the geochemical evolution of groundwater in the Ordovician-Cambrian aquifer system, northern part of the Baltic Artesian Basin. Appl. Geochem. 72, 125–135. https://doi.org/10.1016/j.apgeochem.2016.07.007.
Pärn, J., Affolter, S., Ivask, J., Johnson, S., Kirsimäe, K., Leuenberger, M., Martma, T., Raidla, V., Schloemer, S., Sepp, H., Vaikmäe, R., Walraevens, K., 2018. Redox zonation and organic matter oxidation in palaeogroundwater of glacial origin from the Baltic Artesian Basin. Chem. Geol. 488, 149–161.
Perens, R., Vallner, L., 1997. Water-bearing formation. In: Raukas, A., Teedumäe, A. (Eds.), Geology and Mineral Resources of Estonia. Estonian Academy Publishers, Tallinn, pp. 137–145.
Person, M., McIntosh, J.C., Remenda, V., Bense, V., 2007. Pleistocene hydrology of North America: the role of ice sheets in reorganizing groundwater systems. Rev. Geophys. 45. https://doi.org/10.1029/2006RG000206.
Petersell, V., 1997. Dictyonema argillite. In: Raukas, A., Teedumäe, A. (Eds.), Geology and Mineral Resources of Estonia. Estonian Academy Publishers, Tallinn, pp. 313–326.

Petersen, J.O., Deschamps, P., Hamelin, B., Fourré, E., Gonçalvès, J., Zouari, K., Guendouz, A., Michelot, J.L., Massault, M., Dapoigny, A., Team, A., 2018. Groundwater flowpaths and residence times inferred by ^{14}C, ^{36}Cl and ^{4}He isotopes in the Continental Intercalaire aquifer (North-Western Africa). J. Hydrol 560, 11–23. https://doi.org/10.1016/j.jhydrol.2018.03.003.

Plummer, L.N., Glynn, P.D., 2013. Radiocarbon dating in groundwater systems. In: Isotope Methods for Dating Old Groundwater. IAEA, Vienna, pp. 33–89.

Plummer, L.N., Parkhurst, D.L., Thorstenson, D.C., 1983. Development of reaction models for ground-water systems. Geochem. Cosmochim. Acta 47, 665–685. https://doi.org/10.1016/0016-7037(83)90102-3.

Plummer, L.N., Busby, J.F., Lee, R.W., Hanshaw, B.B., 1990. Geochemical modeling of the Madison-aquifer in parts of Montana, Wyoming and South Dakota. Water Resour. Res. 26, 1981–2014.

Plummer, L.N., Prestemon, E.C., Parkhurst, D.L., 1994. An interactive code (NETPATH) for modeling net geochemical reactions along a flow path, version 2.0. Water-Resources Investig. For. Rep. 94–4169.

Plummer, L.N., Eggleston, J.R., Andreasen, D.C., Raffensperger, J.P., Hunt, A.G., Casile, G.C., 2012. Old groundwater in parts of the upper Patapsco aquifer, Atlantic Coastal Plain, Maryland, USA: evidence from radiocarbon, chlorine-36 and helium-4. Hydrogeol. J. 20, 1269–1294. https://doi.org/10.1007/s10040-012-0871-1.

Raidla, V., Kirsimäe, K., Bityukova, L., Jõeleht, A., Shogenova, A., Šliaupa, S., 2006. Lithology and diagenesis of the poorly consolidated Cambrian siliciclastic sediments in the northern Baltic Sedimentary Basin. Geol. Q. 50, 11–22.

Raidla, V., Kirsimäe, K., Vaikmäe, R., Jõeleht, A., Karro, E., Marandi, A., Savitskaja, L., 2009. Geochemical evolution of groundwater in the Cambrian-Vendian aquifer system of the Baltic Basin. Chem. Geol. 258, 219–231. https://doi.org/10.1016/j.chemgeo.2008.10.007.

Raidla, V., Kirsimäe, K., Vaikmäe, R., Kaup, E., Martma, T., 2012. Applied Geochemistry Carbon isotope systematics of the Cambrian – Vendian aquifer system in the northern Baltic Basin : Implications to the age and evolution of groundwater Gulf of Finland. Appl. Geochem. 27, 2042–2052. https://doi.org/10.1016/j.apgeochem.2012.06.005.

Raidla, V., Kirsimäe, K., Ivask, J., Kaup, E., Knöller, K., Marandi, A., Martma, T., Vaikmäe, R., 2014. Sulphur isotope composition of dissolved sulphate in the Cambrian-Vendian aquifer system in the northern part of the Baltic Artesian Basin. Chem. Geol. 383, 147–154. https://doi.org/10.1016/j.chemgeo.2014.06.011.

Raidla, V., Kern, Z., Pärn, J., Babre, A., Erg, K., Ivask, J., Kalvāns, A., Kohán, B., Lelgus, M., Martma, T., Mokrik, R., Popovs, K., Vaikmäe, R., 2016. A $\delta^{18}O$ isoscape for the shallow groundwater in the Baltic Artesian Basin. J. Hydrol 542, 254–267.

Raidla, V., Aeschbach, W., Weissbach, T., 2017. Noble gases in the Cambrian-Vendian aquifer system in Estonia. PAGES Global Challenges for our Common Future: a paleoscience perspective. Zaragoza, Spain, 9-13 May 2017.

Raudsep, R., 1997. Phosphorite. In: Raukas, A., Teedumäe, A. (Eds.), Geology and mineral resources of Estonia. Estonian Academy Publishers, Tallinn, pp. 331–337.

Raudsep, R., Liivrand, H., Belkin, V., Mardiste, A., Rass, V., Meriküll, V., Madalik, J., Pajupuu, A., Maltseva, I., Semjonova, N., Kelder, N., Kuptsov, A., 1989. Detailed research results from Rakvere phosphorite deposit in Kabala area. Estonian Geology Tallinn. (in Russian).

Saarse, L., Heinsalu, A., Veski, S., 2012. Deglaciation chronology of the Pandivere and Palivere ice-marginal zones in Estonia. Geol. Q. 56, 353–362. https://doi.org/10.7306/gq.1027.

Sanford, W.E., 1997. Correcting for diffusion in carbon-14 dating of groundwater. Gr. Water 35, 357–361.

Savitskaja, L., Viigand, A., Jashtshuk, S., 1995. Report on microcomponent and isotopic composition of groundwater in the Ordovician-Cambrian aquifer system for estimating drinking water quality in north-Estonia. Geological Survey of Estonia, Tallinn. (in Estonian).

Soesoo, A., Hade, S., 2014. Black shales of Estonia: moving towards a Fennoscandian-Baltoscandian database. Transactions of Karelian Research Centre of Russian Academy of Sciences: Precambrian Geology 1, 103–114.

Sterckx, A., Lemieux, J.M., Vaikmäe, R., 2017. Representing glaciations and subglacial processes in hydrogeological models: a numerical investigation. Geofluids 2017, 4598902 12 pages. https://doi.org/10.1155/2017/4598902.

Sterckx, A., Lemieux, J.M., Vaikmäe, R., 2018. Assessment of paleo-recharge under the Fennoscandian Ice Sheet and its impact on regional groundwater flow in the northern Baltic Artesian Basin using a numerical model. Hydrogeol. J. 26, 2793. https://doi.org/10.1007/s10040-018-1838-7.

Stueber, A.M., Walter, L.M., 1991. Origin and chemical evolution of formation waters from Silurian–Devonian strata in the Illinois Basin, USA. Geochem. Cosmochim. Acta 55, 309–325.

Stueber, A.M., Walter, L.M., 1994. Glacial recharge and paleohydrologic flow systems in the Illinois Basin: evidence from chemistry of Ordovician carbonate (Galena) formation waters. Geol. Soc. Am. Bull. 106, 1430–1439.

Suckow, A., 2014. The age of groundwater – Definitions, models and why we do not need this term. Appl. Geochem. 50, 222–230.

Takcidi, E., 1999. Documentation of the Database “Boreholes.” Valsts ģeoloģijas dienests. Riga. (in Latvian).

Tamers, M.A., 1975. Validity of radiocarbon dates on ground water. Geophys. Surv. 2, 217–239. https://doi.org/10.1007/BF01447909.

Torgersen, T., Stute, M., 2013. Helium (and other noble gases) as a tool for understanding long timescale groundwater transport. In: Isotope Methods for Dating Old Groundwater. IAEA, Vienna, pp. 179–216.

Toth, D.J., Katz, B.G., 2006. Mixing of shallow and deep groundwater as indicated by the chemistry and age of karstic springs. Hydrogeol. J. 14, 827–847. https://doi.org/10.1007/s10040-005-0478-x.

Tšeban, E., 1966. Hydrogeology of the USSR XXX (Estonian SSR). VSEGINGEO, Moskow. (in Russian).

Vaikmäe, R., Vallner, L., Loosli, H.H., Blaser, P.C., Juillard-Tardent, M., 2001. Palaeogroundwater of glacial origin in the Cambrian-Vendian aquifer of northern Estonia. Geol. Soc. London, Spec. Publ., London, pp. 17–27. https://doi.org/10.1144/GSL.SP.2001.189.01.03.

Välkmann, S., Savva, V., Otsmaa, M., Boldõreva, N., Simm, D., 1992. Evaluation of groundwater resources in Tartu area. Geological Survey of Estonia, Tallinn (in Estonian).

van der Kemp, W.J.M., Appelo, C.A.J., Walraevens, K., 2000. Inverse chemical modeling and radiocarbon dating of palaeogroundwaters: The Tertiary Ledo-Paniselian aquifer in Flanders, Belgium. Water Resour. Res. 36, 1277–1287. https://doi.org/10.1029/1999WR900357.

Varni, M., Carrera, J., 1998. Simulation of groundwater age distributions. Water Resour. Res. 34, 3271–3281.

Vautour, G., Pinti, D.L., Méjean, P., Saby, M., Meyzonnat, G., Larocque, M., Castro, M.C., Hall, C.M., Boucher, C., Roulleau, E., Barbecot, F., Takahata, N., Sano, Y., 2015. $^{3}H/^{3}He$, ^{14}C and (U-Th)/He groundwater ages in the St. Lawrence Lowlands, Quebec, Eastern Canada. Chem. Geol. 413, 94–106.

Voolma, M., Soesoo, A., Hade, S., Hints, R., Kallaste, T., 2013. Geochemical heterogeneity of Estonian graptolite argillite. Oil Shale 30, 377–401. https://doi.org/10.3176/oil.2013.3.02.

Weissbach, T., 2014. Noble gases in palaeogroundwater of glacial origin in the Cambrian -Vendian aquifer system, Estonia. Master Thesis, University of Heidelberg, Heidelberg.

Wen, T., Castro, M.C., Hall, C.M., Pinti, D.L., Lohmann, K.C., 2016. Constraining groundwater flow in the glacial drift and Saginaw aquifers in the Michigan Basin through helium concentrations and isotopic ratios. Geofluids 16, 3–25.

Whiticar, M.J., 1999. Carbon and hydrogen isotope systematics of bacterial formation and oxidation of methane. Chem. Geol. 161, 291–314. https://doi.org/10.1016/s0009-2541(99)00092-3.

Zuber, A., Weise, S.M., Osenbrück, K., Pajnowska, H., Grabczak, J., 2000. Age and recharge pattern of water in the Oligocene of the Mazovian basin (Poland) as indicated by environmental tracers. J. Hydrol 233, 174–188. https://doi.org/10.1016/S0022-1694(00)00224-9.